CHARACTERIZATION OF AURKA KNOCKOUT IN MOUSE OOCYTES

By

PATRICIA IBRAHIMIAN

A thesis submitted to the

School of Graduate Studies

Rutgers, The State University of New Jersey

In partial fulfillment of the requirements

For the degree of

Master of Science

Graduate Program in Microbiology and Molecular Genetics

Written under the direction of

Karen Schindler

And approved by

_____

_____

_____

New Brunswick, New Jersey

May, 2020

ABSTRACT OF THE THESIS

Characterization of AURKA Knockout in mouse oocytes

By PATRICIA IBRAHIMIAN

Thesis Director:
Karen Schindler

ABSTRACT

Aneuploidy accounts for nearly 30% of all miscarriages and most of these aneuploidies are due to maternal errors during Meiosis I (MI). Cell division in both mitotic and meiotic cells requires proteins that ensure correct chromosome segregation into the resulting daughter cells. In contrast to mitotic cells that have two aurora kinase orthologs, AURKA and AURKB, to help prevent incorrect chromosome segregation, meiosis has an additional AURK, AURKC. In mouse oocytes, AURKA can fully support meiotic maturation by itself in the absence of AURKB/C (Nguyen et al. 2018). To further investigate the essential role of AURKA in oocytes, we analyzed oocyte-specific AURKA knockout (A KO) mice. Surprisingly, we found that A KO female mice are sterile, however, they do ovulate. Furthermore, we demonstrate that, in the absence of AURKA, oocytes cannot form elongated bipolar spindles, complete meiosis I, or extrude a polar body, resulting in oocytes that have arrested at metaphase I (Met I) prior to ovulation. We also determined that this Met I arrest is independent of the spindle assembly checkpoint. Results of these experiments further demonstrate that AURKA is

essential for oocyte meiotic maturation and is required for correct spindle formation and chromosome segregation.

ACKNOWLEDGMENTS

I am so honored to have spent two years in the Schindler lab to conduct research for my Master's project. I am also so grateful to have Dr. Karen Schindler as my advisor and I would like to thank her tremendously for guiding me throughout my entire graduate research journey at Rutgers University, and being an incredible mentor to me and everyone else in the lab. It was not easy being a full time student, researcher, and Teaching Assistant, but Dr. Schindler was always understanding of my busy schedule and supported me through the difficult times, and I am so blessed to have learned so much under her wing.

I would also like to thank the rest of the Schindler lab members. Dr. Cecilia Blengini who first taught me all of the lab techniques and procedures, and helped me acquire the skills needed to work on my research project. She also helped me tremendously when I was overwhelmed and was always there for me whenever I needed someone to talk to for advice. Dr. Mansour Abo-Elenin and Dr. Warif El Yakoubi helped answer my many questions throughout my time in the Schindler lab. Christine Prorock-Rogers for being awesome and always having the genotyping results ready before I needed them. Daniel Jung and Caroline Kratka who walked through this journey with me and became my friends along the way.

Thank you to my committee members, Dr. Karen Schindler, Dr. Kim McKim, and Dr. Ruth Steward for taking time out of their busy schedules to read my thesis and attend my defense.

Thank you to Rutgers University's Microbiology and Molecular Genetics program for giving me this opportunity to conduct great research and learn more than I could have ever imagined in two years.

Thank you to the School of Arts and Sciences General Biology Department for hiring me as a workshop teaching assistant and allowing me to learn so much about teamwork and leadership.

Finally, the biggest thank you to my family members who were there by my side every step of the way and pushing me to be my best. Mom and dad, thank you for being the strongest support system and making sure I was doing well and had everything I needed at all times. My sister and brother, I know you definitely did not know what you were looking at every time I showed you cool confocal images but thank you for still listening to me rant about how pretty they looked. My dear grandpa, thank you for always believing in me, motivating me, and telling me how proud you are of me even when you are on the other side of the world. I could have never become the person I am today and achieved my dreams without all of you being the closest people in my life. I love you always.

TABLE OF CONTENTS

Abstract……ii

Acknowledgements……iv

List of figures……viii

Introduction……..1

Miscarriage and aneuploidy…….1

Mitosis vs meiosis……3

The Aurora Kinases…….7

AURKA's role during cell division…….9

Results……13

Generation and confirmation of mice lacking *Aurka* in oocytes……...13

Aurka conditional knockout female mice are sterile…….……14

Aurka KO oocytes cannot complete meiosis *in vivo* or *in vitro*……14

Loss of AURKA affects phosphorylation levels of INCENP……16

Aurka KO oocyte arrest is SAC independent……17

Results figures and figure legends…….19

Discussion……..29

Materials and methods……...32

Generation of mouse strains and genotyping…….32

Fertility trials……..32

Oocyte collection, culture, and microinjection……..33

Plasmids…….34

Western blotting…….34

Immunocytochemistry……...35

Antibodies……..36

Microscopy……36

Histology……37

Image Analysis……...38

Statistical Analysis…….38

References……..……39

LIST OF FIGURES

Fig 1. Chromosome segregation in the mouse oocyte…….1

Fig 2. Stages of oocyte meiotic maturation…….3

Fig 3. Acentrosomal spindle formation during mouse oocyte Meiosis I…….4

Fig 4. SAC principles during mitotic cell cycle…….……..6

Fig 5. Domains of the Aurora Kinases…….……8

Fig 6. Confirmation of mice lacking *Aurka* in oocytes……..19

Fig 7. *Aurka* conditional knockout female mice are sterile……...21

Fig 8. *Aurka* KO oocytes cannot complete meiosis *in vivo* or *in vitro*……..…23

Fig 9. Loss of AURKA affects phosphorylation levels of INCENP…….25

Fig 10. *Aurka* KO oocyte arrest is SAC independent……27

INTRODUCTION

Miscarriage and aneuploidy

Miscarriage is a major issue that many couples go through while trying to start a family. About 15-20% of pregnancies will result in a spontaneous miscarriage during the first trimester (Jia et al. 2015). Furthermore, 50-80% of early miscarriages are caused by chromosome abnormalities (Petracchi et al. 2009, Menasha et al. 2005). In a recent study analyzing 1,011 cytogenetic results of first trimester miscarriages, chromosome abnormalities were observed in 70.3% of samples with abnormal karyotype (Soler et al. 2017). These abnormalities were mostly aneuploidies which included, but were not limited to, autosomal monosomy/trisomy, X monosomy, triploidy, and tetraploidy. Other abnormal karyotypes included balanced and unbalanced chromosome rearrangements. Aneuploidy is the abnormal number of chromosomes in a cell that result from chromosome mis-segregation (Orr, Godek and Compton 2015). Most cases of human aneuploidy are due to chromosome segregation errors during meiosis I in the egg, and is most frequently associated with increasing maternal age, especially in the decade prior to menopause (Handyside 2012, Franasiak et al. 2014).

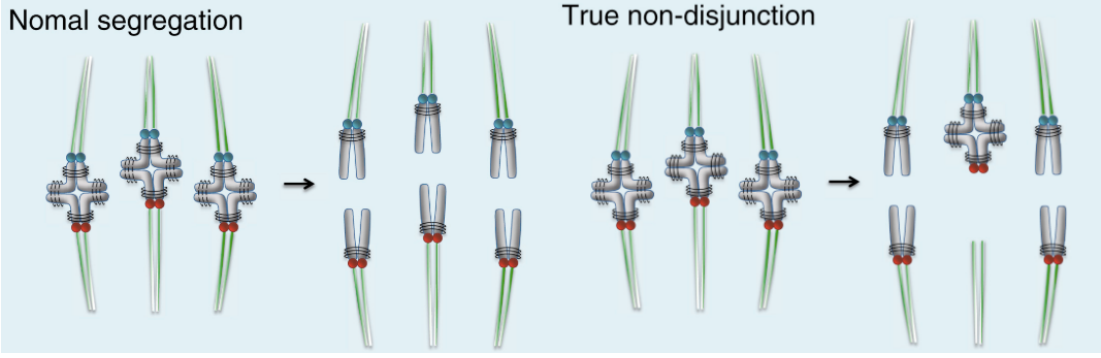

Figure 1. Chromosome segregation in the mouse oocyte. Figure adapted from Mihajlović and FitzHarris 2018. Normal and incorrect homologous chromosome segregation during Meiosis I.

Segregation errors occurring in Meiosis I (MI) are the main cause of aneuploidy and early miscarriages (Chiang, Schultz and Lampson 2012, Nagaoka, Hassold and Hunt 2012). Moreover, recent research revealed that there are three types of errors that compose a U-curve of aneuploidy in females ranging in ages from 9 to 43: 1) Meiosis I nondisjunction increases in patients under the age of 20 , 2) precocious separation of sister chromatids (PSSC) increases linearly in patients over the age of 33, and 3) reverse segregation (RS) increases between the mid and advanced maternal age (AMA) groups (Gruhn et al. 2019). All of these error types result in daughter cells that have an incorrect number of chromosomes after the completion of meiosis. Meiosis is a process where a diploid precursor cell undergoes two rounds of cell division and results in four genetically distinct haploid gametes. In most mammals, oogenesis is initiated in the fetus where the chromosomes in the oocyte undergo replication, pairing, synapsis, and recombination before cell-cycle arrest at Prophase I. Later in the organism's life (i.e. starting at puberty), oocytes will resume meiosis and complete MI by segregating their homologous chromosomes and extruding a polar body before they arrest again at Metaphase II (Met II). The Met II arrest lasts until the egg is fertilized by sperm or until it is discarded during the menstrual cycle (Oliver et al. 2008). This discontinuous meiotic maturation process may cause an increased risk of PSSC due to deterioration of chromosome cohesion that established during fetal development and needs to hold the

sister chromatids together throughout the organism's entire lifetime (Chiang, Schultz and Lampson 2011, Chiang et al. 2010), sometimes up to 50 years.

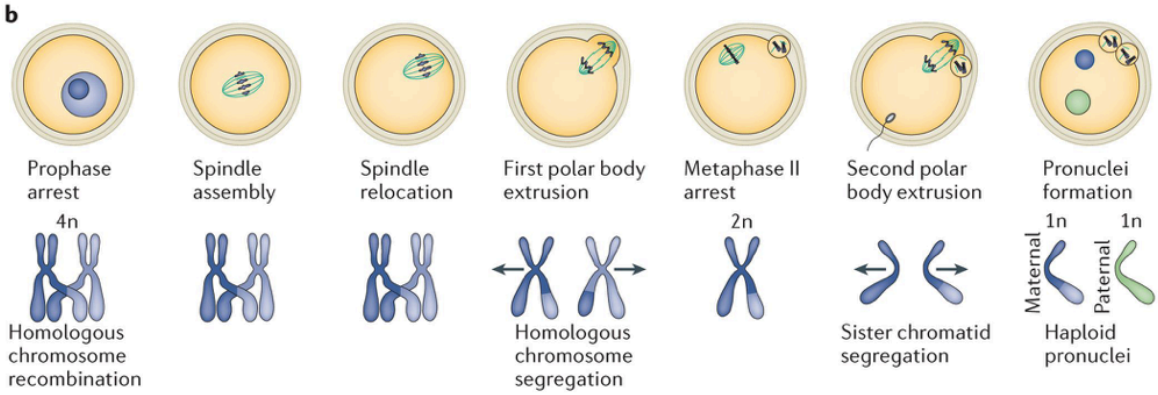

Figure 2. Stages of oocyte meiotic maturation. Figure adapted from Clift and Schuh 2013. First arrest occurs at Prophase and second arrest occurs at metaphase II, following extrusion of a polar body.

Mitosis vs meiosis

Although mitosis and meiosis are both cell division processes that involve segregation of chromosomes, there are differences in the mechanism that they build their spindle in order to segregate the chromosomes. In mitotic cells, centrosomes consist of two centrioles along with pericentriolar matrix proteins, and together they act as major microtubule organization centers (MTOC) that nucleate the microtubules that make up the spindle. They also act as the mitotic spindle poles as they move towards opposite ends of the nuclear envelope to allow the growth and elongation of the microtubules (Bennabi, Terret and Verlhac 2016). The spindle in mammalian oocytes lacks centrioles (Szollosi, Calarco and Donahue 1972). It has multiple clusters of acentriolar MTOCs around the nucleus and in the cytoplasm during the Prophase I arrest (Calarco 2000, Schuh and

Ellenberg 2007, Clift and Schuh 2015). The MTOCs undergo self spindle assembly through multiple MTOCs that functionally replace centrosomes and form from a cytoplasmic microtubule network in prophase (Schuh and Ellenberg 2007, Breuer et al. 2010).

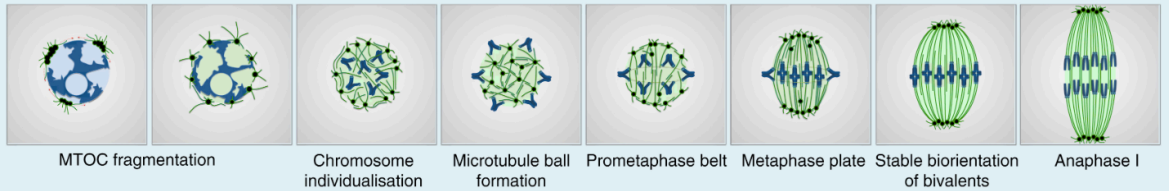

Figure 3. Acentrosomal spindle formation during mouse oocyte Meiosis I. Figure adapted from Mihajlović and FitzHarris 2018. Spindle assembles through multiple MTOCs that form an elongated spindle from Metaphase I to Anaphase I.

Before the oocyte enters the Met I stage, the microtubules need to polymerize so they can attach to the kinetochores that are built at centromeres (Roeles and Tsiavaliaris 2019). Then the oocyte goes through a repeating process of kinetochore-microtubule (K-MT) attachment and detachment until the proper attachments are made and the homologous chromosomes can be correctly segregated towards opposite poles of the spindle (Wollman et al. 2005, Mihajlović and FitzHarris 2018). Once the spindle assembles properly and is ready for the first meiotic division, it is then guided by cytoplasmic actin to position towards the cortex (Field and Lénárt 2011, Azoury et al. 2008, Yi and Li 2012) for the extrusion of half of its homologous chromosomes in its first polar body through asymmetric division (Maddox, Azoury and Dumont 2012, Sun and Kim 2013) thus, completing the first meiotic division.

Because kinetochore-microtubule (K-MT) attachments are error prone, there are checkpoints in both mitosis and meiosis that delay chromosome segregation and cell division until accurate attachments are made. One of these processes is the Spindle Assembly Checkpoint (SAC) (Musacchio and Ciliberto 2012). In mitotic cell division, when the microtubules are not correctly attached to the kinetochores, the Mitotic Checkpoint Complex (MCC) is generated and anaphase onset is inhibited by the anaphase-promoting complex/cyclosome (APC/C) (Sudakin, Chan and Yen 2001) which causes a cell cycle arrest at the Metaphase stage until the attachments are corrected. The MCC includes the Spindle Assembly Checkpoint (SAC) proteins BUBR1, BUB3, CDC20, and MAD2. MAD2 localizes to unattached kinetochores and inhibits the ubiquitination activity of the APC/C along by sequestering its activator protein CDC20, therefore inhibiting anaphase onset (Homer et al. 2005a, Niault et al. 2007). Additionally, disruption of the function of MAD2 prevents normal segregation of homologous pairs (Homer et al. 2005b). The SAC is active when the kinetochores are not correctly occupied by microtubules, causing inhibition of anaphase onset until correct attachments are achieved (Lew and Burke 2003). In contrast, when the SAC is inactive, there are decreased levels of MAD2 on the kinetochores and the APC/C-CDC20 targets degradation of Securin and Cyclin B via ubiquitination (Herbert et al. 2003). Securin is a protein that inhibits Separase, a protease. When Separase is active, it cleaves a subunit of the cohesion complex that is holding the sister chromosomes together leading to their separation in anaphase (Terret et al. 2003, Kudo et al. 2006). During the first meiotic division, the separation of the homologous chromosomes also depends on the APC/C activity and Separase, but centromeric cohesion needs to be protected in order for the

sister chromatids to not separate. Shugoshin-2 (SGO2) localizes to the centromeres and prevents REC8 from being phosphorylated and removing this cohesion (Brar et al. 2006, Kitajima et al. 2006). Because this cohesion is established during embryonic development and needs to hold the sister chromatids for years, sometimes decades, over time, the cohesion weakens and becomes more susceptible to premature separase activation in older oocytes (Chiang et al. 2011). When these oocytes are ready to complete meiosis and be fertilized, the cohesion is not strong enough to hold the sister chromatids together, leading to nondisjunction and aneuploidy in the resulting daughter cell.

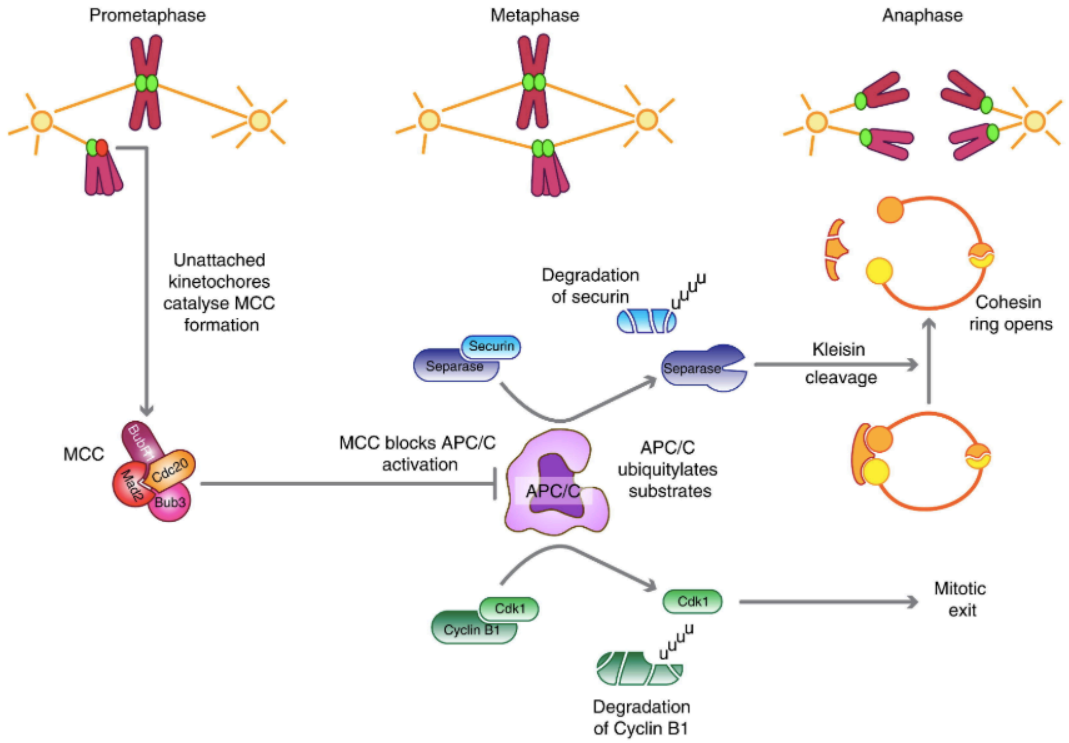

Figure 4. SAC principles during mitotic cell cycle. Figure adapted from Lara-Gonzalez, Westhorpe and Taylor 2012. Unattached kinetochores trigger the formation of the Mitotic Checkpoint Complex (MCC) that will inhibit anaphase onset until the attachment is corrected.

The Aurora Kinases

Meiosis requires precise regulation that involves a number of proteins to ensure it results in healthy gametes. The Aurora Kinases (AURK) are a conserved serine/threonine family that have multiple functions during cell division in both mitosis and meiosis, including spindle assembly, microtubule attachment, and chromosome alignment. These kinases are conserved through multiple species such as *D. melanogaster*, *S. cerevisiae*, and *M. musculus* (Glover et al. 1995, Francisco, Wang and Chan 1994, Shindo et al. 1998). Three auroras are encoded in the mammalian genome: *Aurka*, *Aurkb*, and *Aurkc* (Bischoff and Plowman 1999). *Drosophila melanogaster*, and *C. elegans* have only AURKA and AURKB homologs (Schumacher et al. 1998a, Schumacher, Golden and Donovan 1998b), whereas fungi have one AURK-like homolog (Brown et al. 2004). All three auroras evolved from a single ancestral gene, *IplI*, that was discovered in *S. cerevisiae* (Chan and Botstein 1993) and shares 41% similarity with the human *Aurka* gene. But, it is thought that *Aurkb* and *Aurkc* evolved more recently in mammals through a duplication event (Willems et al. 2018, Brown et al. 2004). Unlike the other Aurora kinases in mammals, AURKC is only expressed in germ cells which sparked a lot of interest due to its expression in meiosis but not mitosis.

In mammals, the three AURKs share about 65-75% similarity in the amino acid sequence of their catalytic domain, which is also conserved across different organisms, but they share little sequence similarity in their N-termini, which may direct their cellular localization and binding to their protein partners (Willems et al. 2018). The functions of the AURKs have been well established in mitosis but their specific roles during oocyte meiotic maturation are still being investigated. AURKA localizes to spindle poles in both

mitosis and meiosis and functions in spindle organization (Saskova et al. 2008, Yao et al. 2004, Eyers et al. 2003). In mitosis, AURKB localizes to the centromeres and has multiple functions such as spindle assembly, cohesion, detection of incorrect K-MT attachments, and cytokinesis (Kelly and Funabiki 2009, Guse, Mishima and Glotzer 2005, Santaguida et al. 2011). In the oocyte, AURKB localizes to the microtubules (Kelly and Funabiki 2009, Balboula and Schindler 2014) and is involved in regulating chromosome alignment (Shuda et al. 2009). Lastly, AURKC is only present in germ cells and is localized at the spindle poles and centromeres/ICA in the oocyte to regulate chromosome alignment and K-MT attachments as well as restrict AURKA to the spindle poles (Balboula and Schindler 2014, Nguyen et al. 2018).

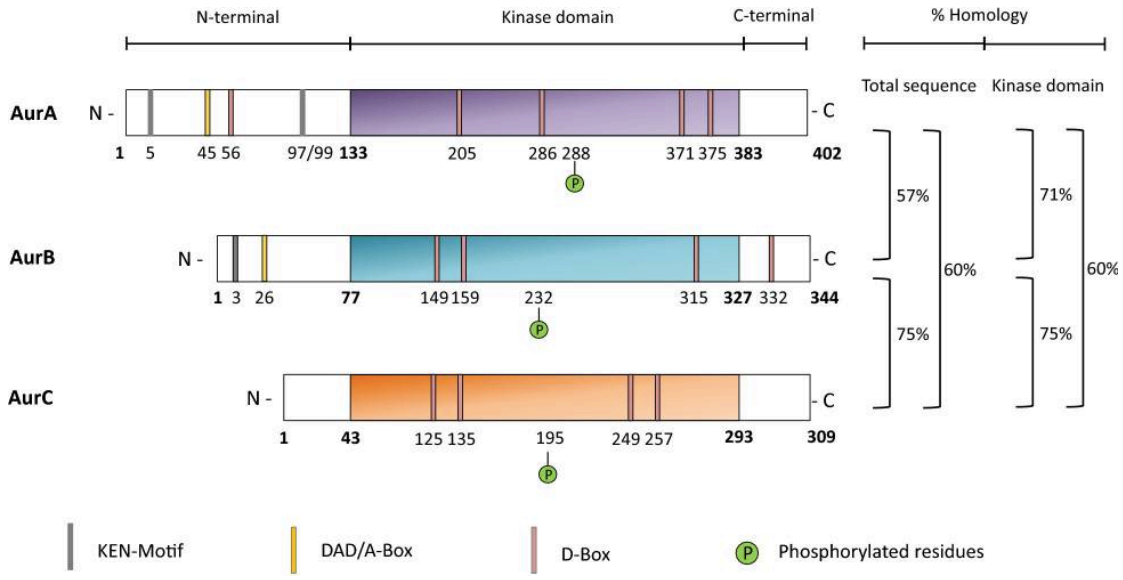

Figure 5. Domains of the Aurora Kinases. Figure adapted from Willems et al. 2018. The three aurora kinases have high sequence conservation in their catalytic domain but little sequence similarities in their N-termini.

AURKA and AURKB/AURKC are activated via auto-phosphorylation that is mediated by cofactors like TPX2 and INCENP, respectively. Previous studies have demonstrated that the microtubule-associated protein TPX2 and Bora are both required for correct localization and activation of AURKA (Eyers et al. 2003, Zhai et al. 2013). Also, mitotic cells that are deficient in the AURKA-TPX2 complex have short spindles and result in mitotic failure despite their ability to successfully segregate the chromosomes (Bayliss et al. 2003). Additionally, we know that AURKB and AURKC act as a catalytic subunit of the chromosomal passenger complex (CPC) in meiosis (Avo Santos et al. 2011), but AURKA can localize to the kinetochores and bind to the CPC in the absence of AURKB and AURKC to compensate for their loss (Nguyen et al. 2018). The CPC is a complex composed of INCENP, Borealin, and Survivin (van der Waal et al. 2012, Kitagawa and Lee 2015). INCENP stimulates auto-phosphorylation and activation of AURKB and AURKC (Bishop and Schumacher 2002). While Borealin and Survivin determine the localization of the complex to the chromosomes (Vader, Maia and Lens 2008, Gassmann et al. 2004).

AURKA's role during cell division

AURKA was discovered in the 1990s while trying to identify genes that control centrosomes and spindle building in *Drosophila* (Glover et al. 1995). It has several important functions during the mitotic cell cycle, and it is an oncogene when its activity is not regulated. In mitosis, AURKA regulates the entry into the cell cycle through phosphorylation of PLK1 and CDC25B (Macůrek et al. 2008, Dutertre et al. 2004). Throughout the mitotic cell cycle stages, AURKA recruits many proteins and factors that

are involved in centrosome maturation (Kinoshita et al. 2005, Mori et al. 2007), stability of microtubules (Asteriti et al. 2011, Zhang, Ems-McClung and Walczak 2008), spindle assembly (De Luca et al. 2008), chromatin driven microtubules nucleation (Pinyol, Scrofani and Vernos 2013), and possibly mitotic cell cycle exit (Marumoto et al. 2003). These functions all occur close to where AURKA is localized throughout the mitotic cell cycle. First, it appears at the centrosomes in late G1 phase and early S phase, then as its expression increases, it localizes to the spindle poles and the adjacent microtubules, and its localization remains associated with the spindle poles throughout telophase (Reboutier, Benaud and Prigent 2015).

The function of AURKA has been well studied in mitosis, but it also has a direct link to multiple cancers. In humans, the *Aurka* locus is at 20q13 which has been identified as a region frequently amplified in breast cancer (Sen, Zhou and White 1997). And when overexpressed, leads to spindle checkpoint disruptions and resistance to anti-mitotic agents (Bischoff et al. 1998, Zhou et al. 1998, Anand, Penrhyn-Lowe and Venkitaraman 2003). This prompted the design of AURKA inhibitors to test their efficiency in preventing tumor growth (Agnese et al. 2007, Carvajal, Tse and Schwartz 2006), and some of these inhibitors like VX-680 and MK-0457 are being tested in clinical trials for their efficacy to repress tumor growth (Giles et al. 2007, Gautschi et al. 2008).

Out of all three mammalian AURKs, AURKA is essential for the progression of meiosis in mouse oocytes (Saskova et al. 2008), is the most abundant, and it can compensate for the loss of the other two AURKs (Nguyen et al. 2018). Therefore, it is important that we have a better understanding of its function during oocyte meiotic

maturation. We know that AURKA co-localizes to the MTOCs during meiosis in mouse oocytes and regulates MTOC number and spindle length. A catalytically inactive form of AURKA is still able to recruit gamma-tubulin to the MTOCs (Solc et al. 2012), which suggests that AURKA has both catalytic dependent and independent functions. Some AURKA inhibitors like MLN8237 have been tested in mouse oocytes to study its effects on chromosome segregation as well as the interactions between AURKA and other proteins (Kovarikova et al. 2016, Komrskova et al. 2014, Nguyen et al. 2018). Inhibition of AURKA and overexpression or reduction of the gene causes distorted spindle organization at Met I and interfered with meiotic resumption (Yao et al. 2004, Saskova et al. 2008). In mitosis, AURKA's role was studied using RNAi but with conflicting results. Some studies show it is required for mitotic commitment (Kunitoku et al. 2003, Hirota et al. 2003) and others show that the cell-cycle arrest that results from inhibition or depletion of AURKA can be bypassed (Yang et al. 2005, Du and Hannon 2004). These inconsistent results call into question what AURKA's true function is during the mitotic and meiotic cell cycles. They also bring up whether the kinase inhibitors that are currently being used in research and to develop anticancer treatments have any effects that are not known yet.

Due to these implications, Cowley and colleagues produced a conditional null allele at the *Aurka* locus in mouse (Cowley et al. 2009). Using this mouse model, they looked at primary embryonic fibroblasts with an *Aurka* deletion and provided further evidence that AURKA is required for mitotic entry. They also showed that the cells that entered prometaphase were monopolar and failed to segregate their chromosomes, and prolonged culture of these cells lead to polyploidy and abnormal nuclear structure.

Additionally, AURKA-deficiency in the germline causes embryonic death at the blastocyst stage. This evidence shows that AURKA is essential for embryonic development and bipolar spindle formation. However, because of embryonic lethality, we do not have the genetic tools to fully assess AURKA requirements.

All of the literature that defines the functions of AURKA in mitosis and meiosis show that it has a key role in spindle formation and chromosome segregation. Because of the high percentage of early miscarriages that are affected by aneuploidy, and the close identity between the mouse and human AURK orthologs, further research of AURKA in mouse oocytes using a conditional knockout model can help us understand its role and involvement in correct chromosome segregation. In this research, we used this conditional knockout model in mouse oocytes and characterized the consequences of deleting *Aurka* during meiotic maturation.

RESULTS

Generation and confirmation of mice lacking *Aurka* in oocytes

Because of AURKA's established key roles in mitotic cell cycle and its noteworthy link to cancers, it is important that we improve our understanding of its role when it comes to meiotic oocyte maturation, specifically because of the high error rate during chromosome segregation. Prior approaches used inhibitors such as MLN8237 and overexpression to investigate AURKA's role in mouse oocyte maturation. We took a genetic approach to investigate the role of AURKA by using the *Gdf9*-mediated Cre excision to create a mouse strain harboring oocytes that lacked *Aurka* (*Aurka*$^{fl/fl}$*;Gdf9-Cre)*. To confirm that AURKA was deleted, we performed immunoblotting and immunocytochemistry. First, we assessed total AURKA. When normalized to the AURKA signal in oocytes from wild-type (WT) littermates, the signal in *Aurka* knockout (A KO) oocytes was absent (Fig. 6A-B). Nonspecific bands were not quantified as part of the AURKA signal. We also assessed the presence of AURKA at Metaphase I (Met I) by immunocytochemistry. A KO oocytes sometimes had short bipolar spindles and other times had collapsed monopolar spindles: a phenotype we will describe in detail later. Compared to WT oocytes, A KO oocytes lacked AURKA signal (Fig. 6C-D). Finally, we measured the activity of AURKA by immunostaining with anti-phosphorylated CDC25B, an AURKA substrate that localizes to spindle poles. Similar to the loss of polar AURKA, there was no detectable pCDC25B in A KO oocytes (Fig. 6E-F). These data support that Gdf9-mediated Cre excision of *Aurka* is sufficient to delete AURKA in mouse oocytes.

Aurka conditional knockout female mice are sterile

To determine the consequence of deleting AURKA in mouse oocytes, we conducted fertility trials. Age-matched WT and A KO females were mated to WT males and the number of pups born was recorded (Fig. 7A). We carried out this fertility trial for the time it took WT females to produce 5 litters. Compared to WT females that produced ~6 pups/litter, A KO females never produced a pup. To investigate if these A KO females ovulate, we examined histological sections of ovaries from these mice at the conclusion of the fertility trial. After quantification of hematoxylin/eosin-stained sections, we found no significant difference in the number of follicles at different developmental stages (Fig. 7B). Importantly, however, we did observe Corpus Luteum (CL) in A KO ovaries, indicating that these females ovulate. The A KO females did have a significant decrease in CL numbers (50% reduced, compared to WT) (Fig. 7C) suggesting that not all oocytes in fully developed follicles were ovulated.

Aurka KO oocytes cannot complete meiosis *in vivo* or *in vitro*

Because A KO females are sterile but ovulate, we wanted to evaluate the meiotic stage of oocytes being ovulated. We therefore harvested cells from oviducts after hormonal stimulation. In this strain background, ~80% of cells in oviducts of WT mice contained polar bodies (Fig. 8A-B), indicating a completion of meiosis I (MI) and arrest at Metaphase of meiosis II (Met II). In contrast, no cells in A KO oviducts had polar bodies suggesting that they are not able to complete meiosis. Further examination of these cells using confocal microscopy showed that compared to WT eggs that had separated their

homologous chromosomes and reached the Met II arrest, A KO oocytes still had intact bivalent chromosomes when ovulated (Fig 8A, zoom).

We also examined *in vitro* maturation of WT and A KO oocytes. Of the WT oocytes isolated and matured *in vitro*, ~60% extruded polar bodies. In contrast, no oocytes isolated from A KO ovaries extruded polar bodies, similar to the oocytes ovulated. Importantly, we did not observe a difference between WT or A KO oocytes resuming meiosis and breaking down the nuclear envelope (~85% vs 80%, WT and A KO, respectively). Further examination of these cells using confocal microscopy also revealed that oocytes from A KO ovaries arrested at Met I whereas oocytes from WT mice reached the Met II arrest (Fig. 8C-E).

To determine when MI becomes abnormal, we examined the cell-cycle events preceding the Met I arrest in A KO oocytes using confocal microscopy. We matured the oocytes for the time it took the WT oocytes to reach early prometaphase I (3h), late prometaphase I (5h), and Met I (7h) stages *in vitro* (Fig. 8F-H). When WT oocytes transition from prometaphase I to Met I, the spindle becomes bipolar and elongates until two distinct poles form and chromosomes align at the metaphase plate. In contrast, the A KO oocytes had a collapsed spindle at the early prometaphase stage and the spindle either remained collapsed with one pole or elongated slightly at the late prometaphase stage to form a short bipolar spindle. Interestingly, spindles in A KO oocytes did not elongate further once oocytes reached the Met I stage, and they were either collapsed monopolar or short bipolar spindles. When we quantified these two spindle phenotypes that we observed in A

KO oocytes, ~55% had monopolar spindles, and ~45% had short bipolar spindles after 7h of meiotic maturation (Fig. 8I). Furthermore, when spindle measurements were compared between A KO and WT spindles, A KO oocytes had significantly shorter bipolar spindles (averages of 29.54 μm vs 15.92 μm, WT and A KO, respectively) and bipolar spindle areas (averages of 615.9 μm^2 vs 205.0 μm^2, WT and A KO, respectively) compared to WT oocytes (Fig. 8J-K).

Because A KO oocytes had abnormal spindle morphology and misaligned chromosomes, we wanted to examine meiotic maturation in real time using high-resolution live-cell imaging. WT and A KO oocytes were microinjected with H2B-mCherry and mEGFP-CDK5RAP2 to visualize the chromosomes and MTOCs, and incubated with SiR-tubulin to visualize the microtubules. Prior to nuclear envelope breakdown, WT oocytes had fragmented MTOCs in the cytoplasm and at poles that then clustered together to form two distinct spindle poles at Met I (Fig. 8L). A KO oocytes instead had only 1 to 2 MTOCs that migrated around the chromosomes. These few MTOCs did not form two poles to segregate the chromosomes, resulting in a failure to extrude a polar body.

Loss of AURKA affects phosphorylation levels of INCENP

We previously showed that inhibition of AURKA using MLN8237 in AURKB and AURKC double knockout oocytes resulted in the loss of phosphorylated INCENP (pINCENP) (Nguyen et al, 2018), implying that AURKA can bind INCENP, a CPC component, by itself and compensate for the loss of AURKB/C. Furthermore, recent work in HeLa cells indicates that AURKA binds INCENP even in the presence of

AURKB (DeLuca 2017, DeLuca et al. 2018). We wanted to assess whether AURKA can phosphorylate INCENP using immunostaining. When normalized to the pINCENP signal in WT oocytes, the signal in monopolar and bipolar A KO oocytes was decreased by ~50% and ~25%, respectively (Fig. 9A-B). Changes in pINCENP pixel signal upon deletion of *Aurka* motivated us to examine the levels of activated AURKC (pAURKC) using immunoblotting. We used a phospho-specific antibody to detect total pAURKC in WT and A KO oocytes. Importantly, we did not observe any changes in total activated protein levels (Fig. 9C-D). These data suggest that AURKA does not regulate AURKC activity and suggest that AURKA can bind and phosphorylate INCENP in WT oocytes.

Aurka KO oocyte arrest is SAC independent

Finally, we wanted to determine the cause of the failure to extrude a polar body. Insufficient tension between kinetochores and microtubules (K-MT) activates an error-correction pathway involving AURKB/C which triggers detachment of MTs. This loss of attachments activates the SAC (Vallot et al. 2018) and results in cell-cycle arrest preventing anaphase. We suspected that the arrest in the A KO oocytes was due to a lack of tension from monopolar spindles. We investigated the strength of SAC activity in MI by evaluating MAD2 signals at kinetochores using confocal microscopy (Fig. 10A). When normalized to MAD2 signal in WT oocytes, monopolar A KO oocytes had significantly higher MAD2 signal. In contrast, the A KO oocytes with short bipolar spindles had levels of MAD2 closer to WT (Fig. 10B). These data suggest that the SAC blocks anaphase onset in A KO oocytes with monopolar spindles, likely due to a loss of tension.

Next, to assess whether the Met I arrest in A KO oocytes is SAC dependent, we treated oocytes with Reversine to inhibit monopolar spindle 1 (MPS1) kinase, a core SAC protein required for initiating the SAC signaling complex (Hached et al. 2011), and monitored polar body extrusion live (Fig. 10C). About 10h after meiotic maturation, WT oocytes in DMSO started to extrude polar bodies (Fig. 10D), whereas A KO oocytes in DMSO failed to extrude polar bodies. On average, 64% of WT oocytes had polar bodies in DMSO, which increased to ~93% upon Reversine treatment. Consistent with previous reports, addition of Reversine increases the kinetics of the cell cycle and polar body extrusion (Collins et al. 2015). The percent of polar body extrusion in A KO oocytes increased from 0% in DMSO to ~19% when treated with Reversine. Interestingly, further examination of these cells using confocal microscopy revealed that the A KO oocytes that extruded polar bodies still had misaligned chromosomes and short bipolar spindles (Fig. 10E). These Met II phenotypes were never observed in WT eggs. The significant percentage of A KO oocytes that failed to extrude a polar body in Reversine suggest that the Met I arrest is SAC independent.

RESULTS FIGURES AND FIGURE LEGENDS

Figure 6

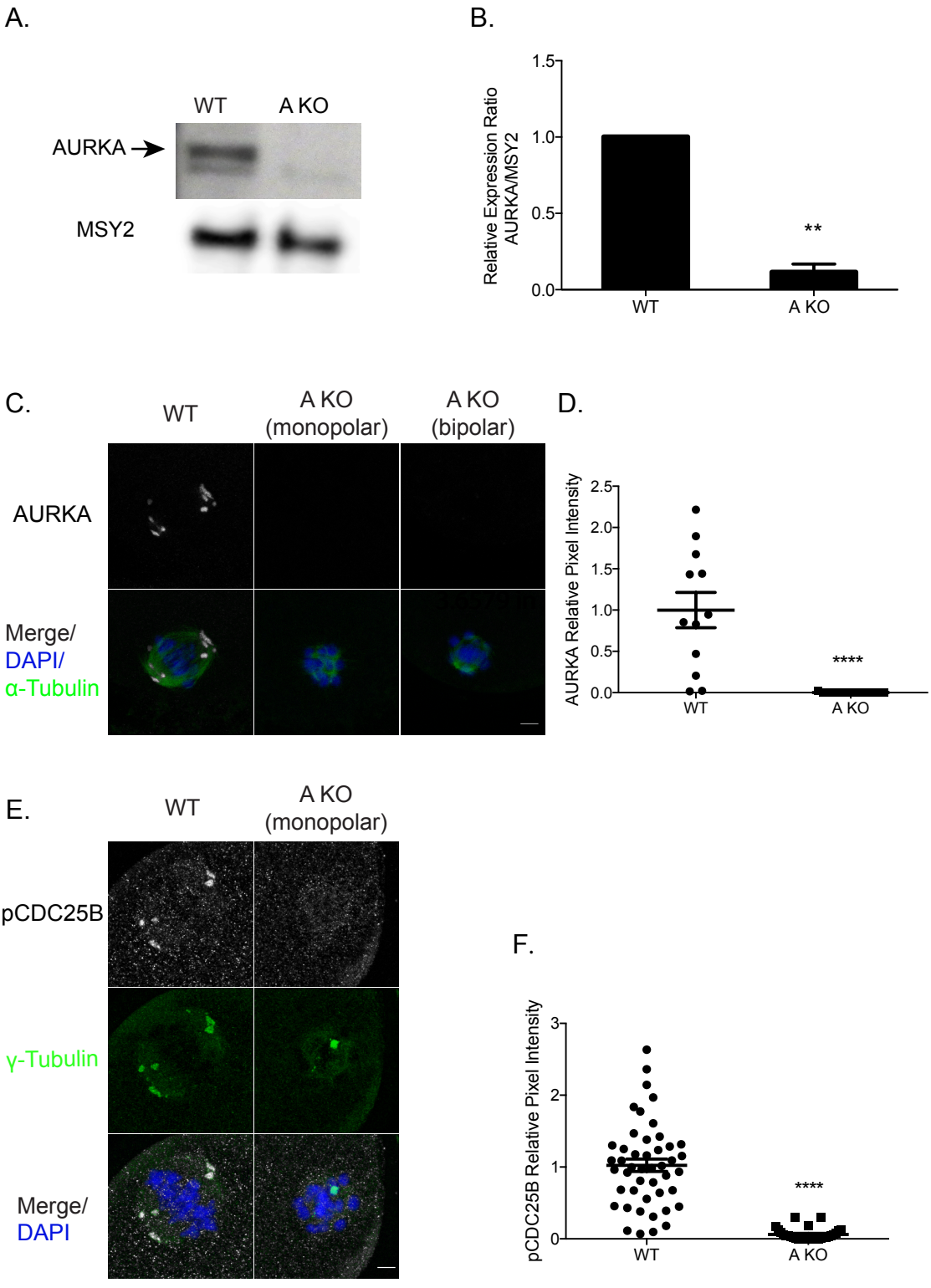

Fig. 6 Confirmation of mice lacking *Aurka* in oocytes. A) Western blot of AURKA from prophase-I arrested WT and A KO oocytes. (100 oocytes/lane). MSY2 served as loading control. Bands at ~43kDa in both WT and A KO lanes were included in the quantifications for AURKA signal. n=4 animals/genotype/experiment. two experimental replicates performed. B) Values normalized to MSY2 from A. C-E) Representative confocal z-projections of Metaphase I WT and A KO oocytes. C) Cells stained for AURKA (gray), spindle (α-tubulin, green), and DNA (DAPI, blue). D) Relative pixel intensity of AURKA, normalized to WT, from C. Each data point is from a single oocyte. E) Cells stained for pCDC25B (gray), poles (γ-tubulin, green), and DNA (DAPI, blue). F) Relative pixel intensity of pCDC25B, normalized to WT, from E. Each data point is from a single oocyte with two experimental replicates performed. **p = 0.0035; ****p = <0.0001; Scale bar = 5 μm.

Figure 7

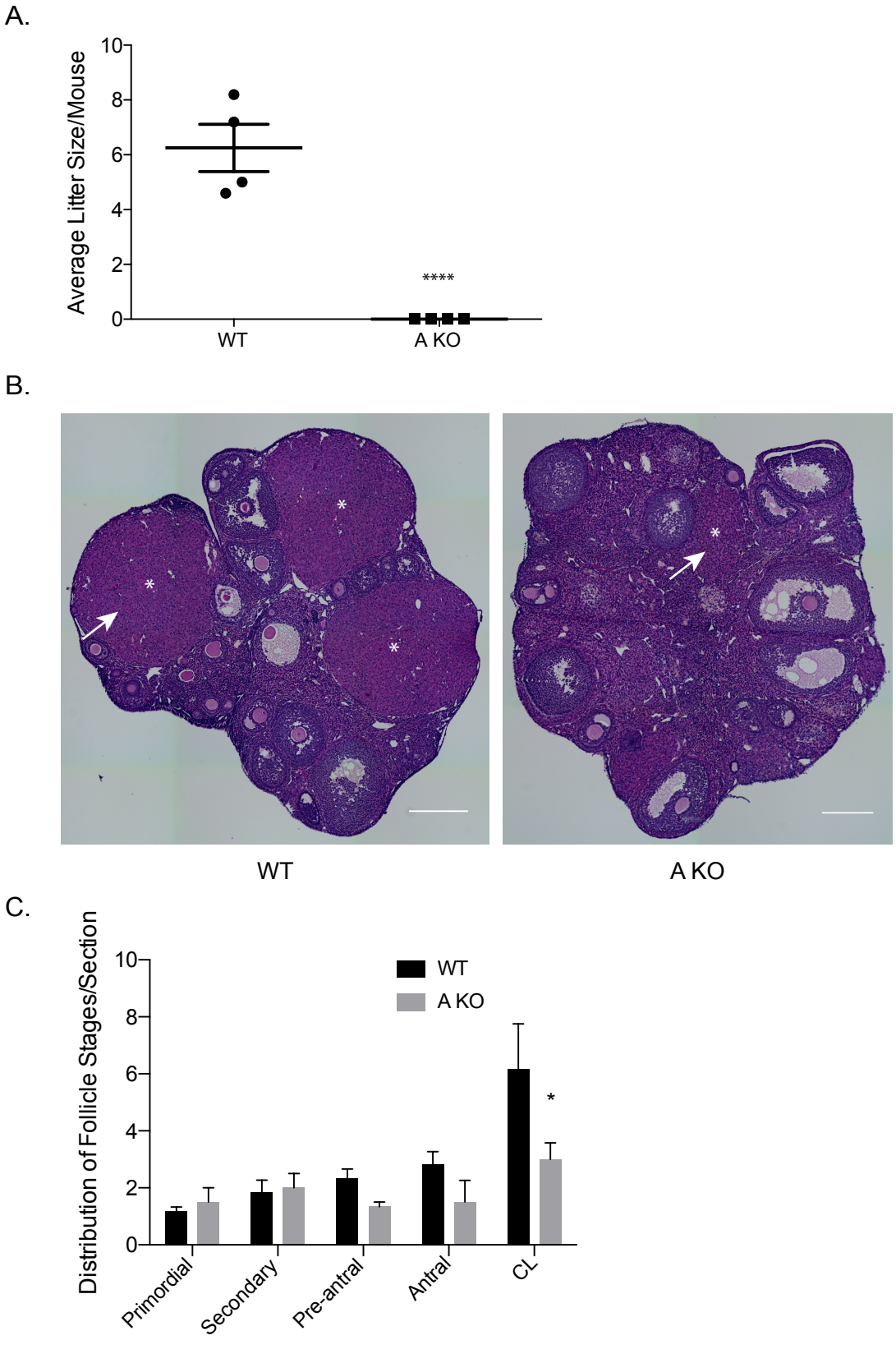
A.
Average Litter Size/Mouse
10
8
6
4
2
0
****
WT
A KO
B.
WT
A KO
C.
Distribution of Follicle Stages/Section
10
8
6
4
2
0
WT
A KO
*
Primordial
Secondary
Pre-antral
Antral
CL

Fig. 7 ***Aurka*** **conditional knockout female mice are sterile.** A) Average litter size from fertility studies. Age-matched WT and A KO female mice. The number of pups/5 litters was recorded. n=4 animals/genotype. B) Representative images of hematoxylin/eosin-stained (HE) ovarian sections from WT and A KO female mice from A. Asterisks and arrow denote Corpus Luteum. C) Quantifications of the stages of folliculogenesis from B. *p = 0.0269; Scale bar = 200 μm.

Figure 8

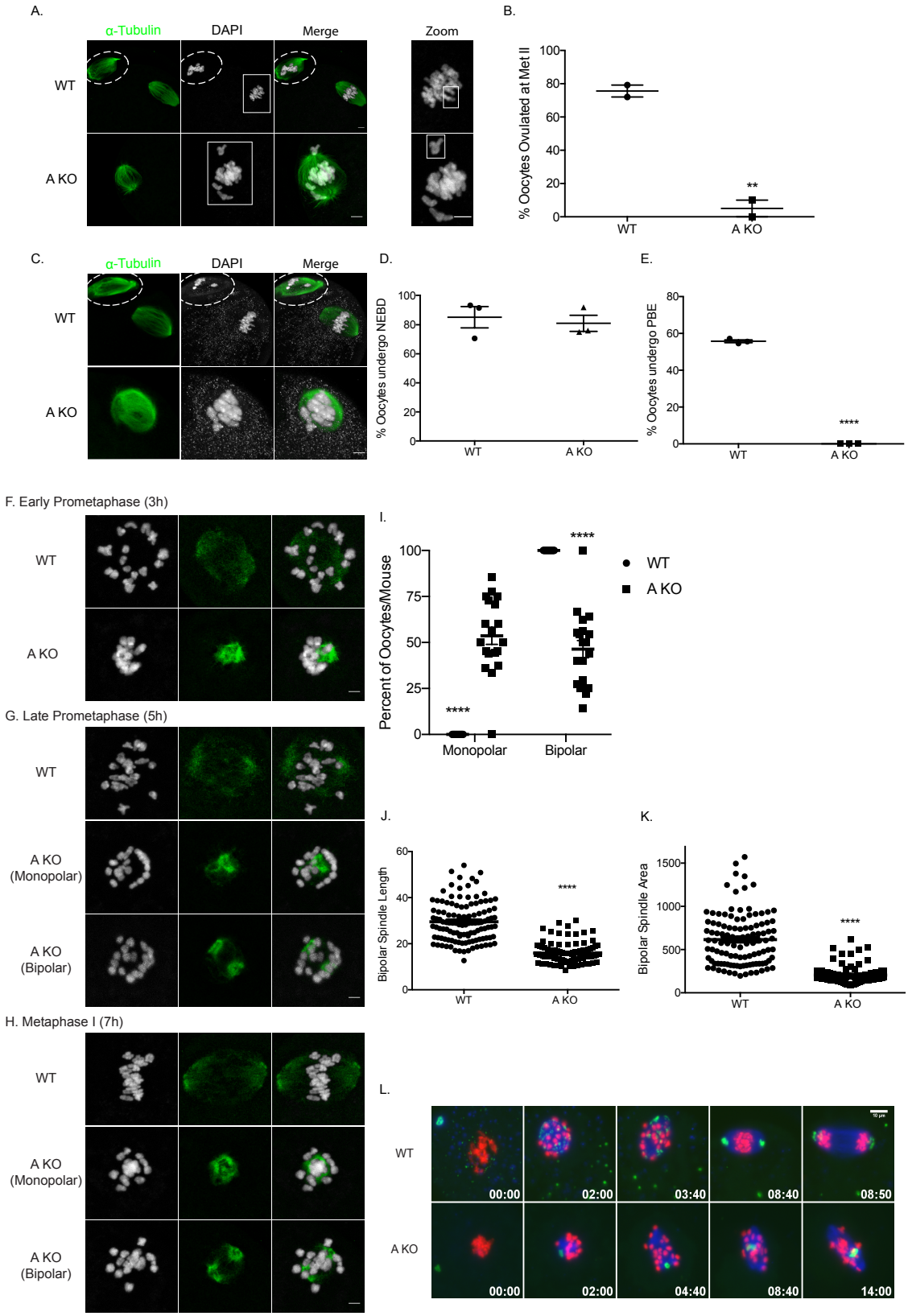
A.
α-Tubulin
DAPI
Merge
Zoom
WT
A KO
B.
% Oocytes Ovulated at Met II
100
80
60
40
20
0
**
WT
A KO
C.
α-Tubulin
DAPI
Merge
WT
A KO
D.
% Oocytes undergo NEBD
100
80
60
40
20
0
WT
A KO
E.
% Oocytes undergo PBE
80
60
40
20
0
****
WT
A KO
F. Early Prometaphase (3h)
WT
A KO
G. Late Prometaphase (5h)
WT
A KO
(Monopolar)
A KO
(Bipolar)
H. Metaphase I (7h)
WT
A KO
(Monopolar)
A KO
(Bipolar)
I.
Percent of Oocytes/Mouse
100
75
50
25
0
****
****
Monopolar
Bipolar
WT
A KO
J.
Bipolar Spindle Length
60
40
20
0
****
WT
A KO
K.
Bipolar Spindle Area
1500
1000
500
0
****
WT
A KO
L.
WT
00:00
02:00
03:40
08:40
08:50
A KO
00:00
02:00
04:40
08:40
14:00

Fig. 8 ***Aurka*** **KO oocytes cannot complete meiosis** ***in vivo*** **or** ***in vitro.*** A) Representative confocal z-projections of ovulated cells from hormonally induced WT and A KO mice were stained for spindle (α-tubulin, green), and DNA (DAPI, gray). B) Percent oocytes ovulated at Metaphase II *in vivo* from A. n = 2 animals/genotype. C) Representative confocal z-projections of Met II WT and A KO cells matured *in vitro* and stained for spindle (α-tubulin, green), and DNA (DAPI, gray). D-E) Percent oocytes undergo nuclear envelope breakdown (NEBD) and percent oocytes undergo polar body extrusion (PBE), respectively, from C. n = 3 animals/genotype. F-H) Representative confocal z-projections from Prophase I arrested oocytes from WT and A KO mice matured *in vitro* to Early Prometaphase (3h), Late Prometaphase (5h), and Metaphase I (7h), respectively. Cells were stained for spindle (α-tubulin, green), and DNA (DAPI, gray). I) Percent oocytes that are monopolar vs bipolar. n = 19 animals/genotype. J-K) Quantifications of bipolar spindle length and bipolar spindle area, respectively. n = 11 animals/genotype. L) Snapshots of live-imaged oocytes after microinjection with H2B-mCHERRY and mEGFP-CDK5RAP2 and incubated with SiR-tubulin. Dotted circles denote polar bodies. Squares denote area of zoom. **p = 0.0075; ****p = <0.0001; Scale bar = 5 μm for A-H, and 10 μm for L.

Figure 9

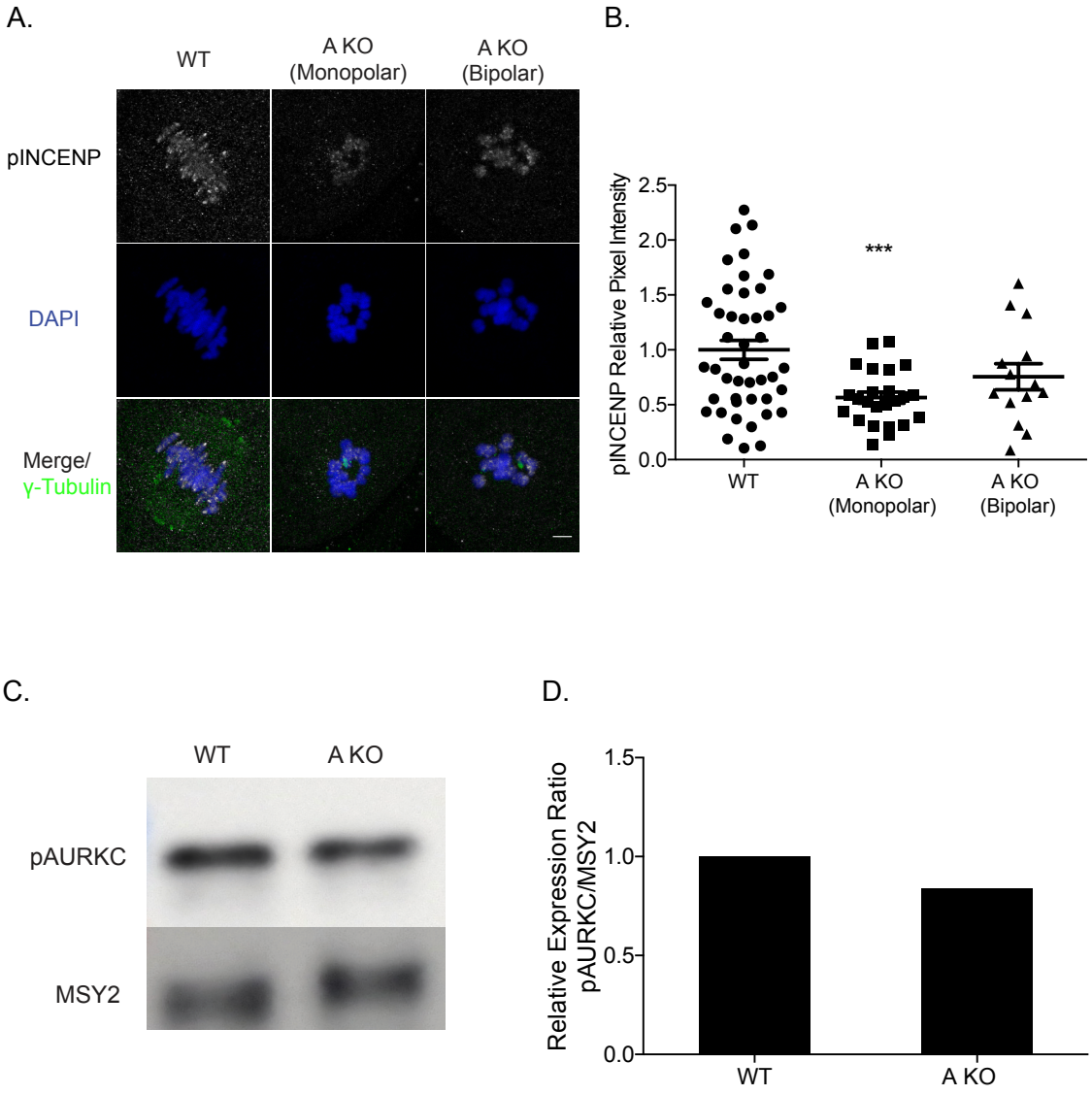
A.
WT
A KO (Monopolar)
A KO (Bipolar)
pINCENP
DAPI
Merge/ γ-Tubulin
B.
pINCENP Relative Pixel Intensity
2.5
2.0
1.5
1.0
0.5
0.0
***
WT
A KO (Monopolar)
A KO (Bipolar)
C.
WT
A KO
pAURKC
MSY2
D.
Relative Expression Ratio pAURKC/MSY2
1.5
1.0
0.5
0.0
WT
A KO

Fig. 9 Loss of AURKA affects phosphorylation levels of INCENP. A) Representative confocal z-projections of Met I oocytes stained for pINCENP (gray), poles (γ-tubulin, green), and DNA (DAPI, blue). n = 3 animals/genotype. B) pINCENP pixel intensity relative to WT. C) Western blot of pAURKC from WT and A KO oocytes matured to Met I (91 oocytes/lane). MSY2 served as loading control. n=3 animals/genotype/experiment. D) Values normalized to MSY2 from A.***p = 0.0008. Scale bar = 5 μm.

Figure 10

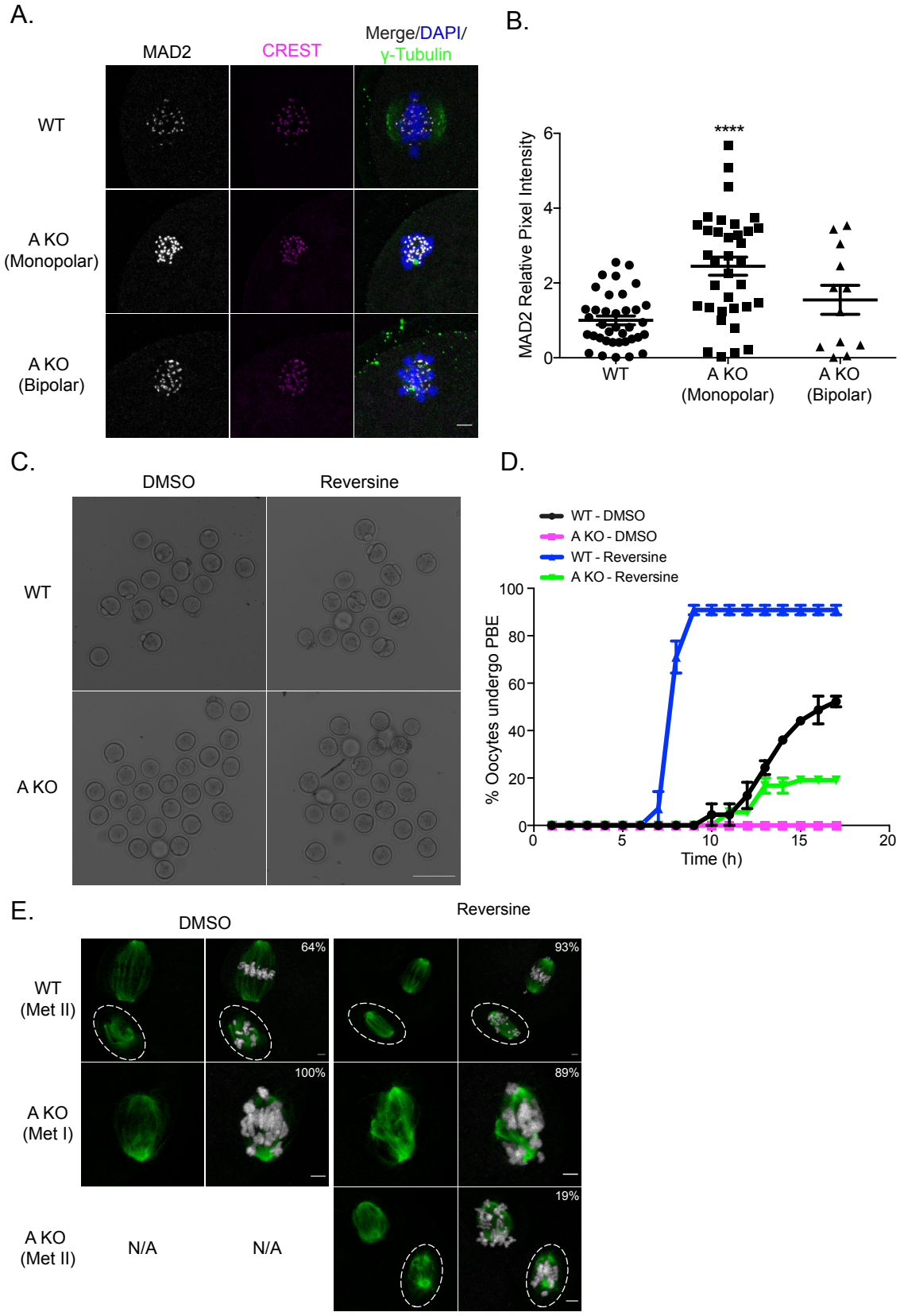
A.
MAD2
CREST
Merge/DAPI/
γ-Tubulin
WT
A KO
(Monopolar)
A KO
(Bipolar)
B.
MAD2 Relative Pixel Intensity
****
WT
A KO
(Monopolar)
A KO
(Bipolar)
C.
DMSO
Reversine
WT
A KO
D.
WT - DMSO
A KO - DMSO
WT - Reversine
A KO - Reversine
% Oocytes undergo PBE
Time (h)
E.
DMSO
Reversine
WT
(Met II)
A KO
(Met I)
A KO
(Met II)
64%
93%
100%
89%
19%
N/A
N/A

Fig. 10 ***Aurka*** **KO oocyte arrest is SAC independent.** A) Representative confocal z-projections of Met I cells stained for MAD2 (gray), CREST (magenta), spindle (γ-tubulin, green), and DNA (DAPI, blue). B) MAD2 pixel intensity in monopolar and bipolar A KO oocytes separately, relative to WT. n = 4 animal/genotype. C) Live image snapshots of WT and A KO Met II eggs matured in the presence of the indicated drug. n = 2 animal/genotype. D) Percent of oocytes from C able to undergo PBE. E) Eggs from C were fixed and stained for spindle (α-tubulin, green), and DNA (DAPI, gray). ****p = <0.0001. Scale bars = 5 μm in A-D and 200 μm in C.

DISCUSSION

Consistent with previous research documenting AURKA's importance to bipolar spindle formation and meiosis completion (Saskova et al. 2008, Solc et al. 2012, Cowley et al. 2009), here we show that conditional deletion of *Aurka* in mouse oocytes results in spindle defects and Met I arrest. Our previous finding showed that mice with *Aurkb* and *Aurkc* double KO oocytes were still fertile, indicating that AURKA can support meiotic maturation without the other AURKs (Nguyen et al. 2018). For the first time, we show that *Aurka* KO mice are sterile, but can ovulate. Despite our efforts to harvest ovulated Met II A KO eggs, as well as to mature A KO oocytes from prophase I to Met II *in vitro*, A KO oocytes always arrested at Met I and failed to extrude a polar body. Moreover, A KO oocytes displayed two extreme spindle phenotypes when matured to Met I (7h): monopolar spindle and short bipolar spindle.

To our surprise, although MAD2 appeared to be significantly increased in the monopolar A KO oocytes, SAC activity was not the only reason that they arrested before extruding a polar body. When we inhibited the activity of the SAC with Reversine, only 19% of A KO oocytes extruded polar bodies. Additionally, because A KO oocytes do not extrude polar bodies, we were unable to completely assess details of AURKA's role beyond chromosome segregation using this KO model. Furthermore, our previous research using the AURKA inhibitor MLN8237 in double KO oocytes showed evidence that AURKA can phosphorylate INCENP in a CPC-dependent manner by migrating some of its population to the chromosomes (Nguyen et al. 2018). In this KO model, we showed supporting results that AURKA phosphorylates INCENP. However, similar to the MAD2

findings, the pINCENP signal intensity only in the monopolar A KO oocytes appeared to be different from the WT oocytes.

Additionally, because AURKA is responsible for phosphorylating a number of other proteins that are involved in regulating the mitotic centrosome, spindle, K-MT attachments, as well as maintenance of sister chromatid cohesion, it should be considered that the deletion of *Aurka* in the mouse oocyte affected the activation of these substrates, leading to extreme spindle phenotypes and cell cycle arrest. For example, an AURKA substrate, Polo-Like Kinase 1(PLK1), is activated during the resumption of meiosis in the mouse oocyte and promotes the formation of acentriolar bipolar spindles (Solc et al. 2015), which may explain the two spindle phenotypes that are present in the A KO oocytes. Moreover, when PLK1 is inhibited in mouse oocytes, the APC/C is not activated, independent of satisfying the SAC, leading to a Met I arrest (Solc et al. 2015). If PLK1 is not phosphorylated by AURKA but is required for full activation of APC/C, then this may explain the SAC independent arrest in A KO oocytes.

Furthermore, other AURKA substrates involved in centrosome maturation, spindle/MT growth, and spindle orientation include CPAP, TACC and Kif18, and PAR6 and NuMA, respectively (Magnaghi-Jaulin et al. 2019). Because of AURKA's extensive role in phosphorylating a number of proteins that have multiple functions in ensuring the cell maturation occurs precisely, it is very likely that the deletion of *Aurka* results in a downstream disturbance of its substrates, leading to multiple chromosome, spindle, and MTOC defects, as we see in our A KO model.

Based on what we know from previous research about AURKA's many functions in mitosis from centrosome maturation and spindle assembly, to cell cycle exit, and its involvement in forming the MTOCs in the mouse oocyte, it is not surprising that a deletion of the *Aurka* gene in mouse oocytes results in faulty MTOC formation and spindle defects. However, what is surprising is that AURKB/C cannot compensate for AURKA's loss and the result is a meiotic cell cycle arrest. Because AURKB/C are less abundant than AURKA in WT oocytes, this lack of compensation leads us to wonder whether an overexpression of AURKB/C in A KO oocytes will lead to some degree of cell cycle rescue.

AURKA has a key role in oocyte meiotic maturation and our findings provide new insights about the degree of its importance during female meiosis. We show that AURKA's function is important for forming an elongated bipolar spindle, correctly segregating chromosomes, and reaching the Met II stage. Because of AURKA's important roles during meiosis and the high percentage of aneuploidy causing early miscarriages, this work is relevant for the reproductive field as it helps us understand the mechanism of chromosome segregation and why mammalian meiosis requires all three AURKs when AURKA by itself is sufficient to complete meiotic maturation. It is therefore crucial that we understand the contributions that AURKA and the other AURKs plays in generating a healthy egg.

MATERIALS AND METHODS

Generation of mouse strains and genotyping

Mice possessing *loxP* sites on either side of exon 2 of the *Aurka* gene (Cowley et al. 2009) were purchased from Jackson Laboratories (B6.129-*Aurka*$^{tm1.1Tvd}$/J, #017729). To generate *Aurka*$^{fl/fl}$ Gdf9-Cre mice, female mice carrying the *Aurka* floxed alleles were crossed with Gdf9-Cre males (Jackson Laboratories Tg(Gdf9-icre)5092Coo/J, #011062). Genotyping for LoxP and Cre were carried using PCR amplification. Primers for *Aurka LoxP* (Forward: 5' - CTGGATCACAGGTGTGGAGT- 3', Reverse: 5' – GGCTACATGCAGGCAAAC A - 3'), and *Gdf9-Cre* (Forward: 5' - TCTGATGAAGTCAGGAAGAAC C- 3', Reverse: 5' - GAGATGTCCTTCACTCTGATT C-3', Internal control Forward: 5' - CTAGGCCACAGAATTGAAAGATCT- 3', Internal control Reverse: 5' - GTAGGTGGA AATTCTAGCATCATC C- 3') were used at 20 pMol using FastMix French PCR beads (Bulldog Bio, #25401) following manufacturers protocol.

Fertility trials

Sexually mature wild-type *Aurka*$^{fl/fl}$ and *Aurka*$^{fl/fl}$;Gdf9-Cre (A KO) female mice ages 5 to 13 weeks were continuously mated to wild type B6D2 (Jackson Laboratories B6D2F1/J, #100006) male mice with proven fertility until a total of 5 litters were produced by wild type female mice. Average age of female mice at the end of the fertility trials was 7 months.

Oocyte collection, culture, and microinjection

Fully grown, prophase I-arrested oocytes were collected from the ovaries of mice ranging in age from 3 to 12 weeks. To prevent spontaneous meiotic resumption during collection, 2.5 μM milrinone (Sigma-Aldrich #M4659) was added to minimal essential medium (MEM). To induce meiotic resumption, oocytes were cultured in milrinone-free Chatot, Ziomek, and Bavister (CZB) (Chatot et al. 1989) medium in an atmosphere of 5% CO_2 in air at 37 °C. Oocytes were matured for 7.5 hours for metaphase I experiments and 16 hours for Metaphase II experiments.

For induced ovulation and collection of metaphase II eggs, female mice (>6 wks. age) were injected with 150 μL of pregnant mare's serum gonadotropin (PMSG) (Lee Biosolutions #493-10) followed by 150 μL of human choronic gonadotropin (hCG) (Sigma-Aldrich #CG5) 47 h later. 14-16 h post hCG injection, eggs were collected from the oviducts in MEM/polyvinylpyrrolidone media containing 3 mg/ml hyaluronidase (Sigma-Aldrich, #H3506) in MEM for 5 min. Eggs were then washed free of hyaluronidase and allowed to recover in MEM/polyvinylpyrrolidone media prior to fixation.

For *in vitro* maturation of drug-treated oocytes, Reversine (Cayman Chemical Research #10004412) was added to CZB culture media at a final concentration of 0.5 μM. Dimethyl sulfoxide (Sigma Aldrich #472301) was used as a control in the same dilution factor (1:2,000). Oocytes were matured in a 96-well plate (ThermoFisher Scientific #269620) using an EVOS FL Auto Imaging System (Life Technologies) with a 20×

objective. The microscope stage was heated to 37 °C and 5% CO2 was maintained using the EVOS Onstage Incubator.

Oocytes were microinjected in M2 medium (Sigma-Aldrich #M7167) with ~10 pl of 50 ng/ml H2B-mCherry (Kitajima, Ohsugi and Ellenberg 2011), 125 ng/ml mEGFP-CDK5RAP2 (Balboula et al. 2016). Oocytes were stained with 100 nM SiR-tubulin (Spirochrome #SC002) for microtubule visualization SiR-tubulin was added to MEM medium. Microinjected oocytes were cultured for 3h in MEM medium supplemented with milrinone to allow protein expression.

Plasmids

To generate cRNA, plasmids were linearized and in vitro transcribed using a mMessage mMachine T3 (Ambion #AM1348) and T7 kits (Ambion #AM1344), according to manufacturer's protocol. The synthesized cRNAs were then purified using an RNAeasy kit (Qiagen #74104) and stored at -80 °C.

Western blotting

A total of 100 pooled prophase-I arrested oocytes were mixed with Laemmli sample buffer (Bio-Rad, cat #161-0737) and denatured at 95°C for 10 min. Proteins were separated by electrophoresis in 10% SDS polyacrylamide precast gels (Bio-Rad, #456-1036, Hercules, USA). The separated polypeptides were transferred to nitrocellulose membranes (Bio-Rad, #170-4156) using a Trans-Blot Turbo Transfer System (Bio-Rad) and then blocked with 2% ECL blocking (Amersham, #RPN418) solution in TBS-T

(Tris-buffered saline with 0.1% Tween 20) for at least 1h. The membranes were incubated overnight using the antibody dilution anti-AURKA (1:500; Bethyl #A300-072A), anti-pAURKA/B/C (1:500; Cell Signaling #2914S), or 1 hr with anti-MSY2 (1:20,000; gift from R. Schultz) as a loading control. After washing with TBS-T five times, the membranes were incubated with anti-rabbit secondary antibody (1:1000; Kindle Bioscience, #R1006) for 1 h followed with washing with TBS-T five times. The signals were detected using the ECL Select western blotting detection reagents (Kindle Bioscience, #R1002) following the manufacturers protocol. Membranes were stripped prior to loading control detection using Blot Stripping Buffer (ThermoFisher Scientific #46430) for 30 minutes at room temperature.

Immunocytochemistry

Following meiotic maturation, oocytes were fixed in PBS containing paraformaldehyde (PFA) at room temperature (CREST, α-tubulin, pCDC25B, AURKC, pAURKA/B/C, and pINCENP: 2% PFA for 20 mins; pAURKA: 2% PFA + 0.1% Triton-X for 20 mins; γ-tubulin: 3.7% PFA for 20 minutes) or PHEM (PIPES 60mM, HEPES 25mM, EGTA 10mM, and $MgCl_2$ 2mM) containing paraformaldehyde (MAD2: 2% PFA for 20 mins) followed by 3 consecutive washes through blocking buffer (PBS + 0.3% (wt/vol) BSA + 0.1% (vol/vol) Tween-20). Prior to immunostaining, oocytes were permeabilized for 20 min in PBS containing 0.1% (vol/vol) Triton X-100 and 0.3% (wt/vol) BSA followed by 10 min in blocking buffer. Immunostaining was performed by incubating cells in primary antibody for 1 h in a dark humidified chamber at room temperature followed by 3 consecutive 10 min incubations in blocking buffer. After washing, secondary antibodies

were diluted 1:200 in blocking solution and the sample was incubated for 1 h at room temperature. After washing, the cells were mounted in 5 μL VectaShield (Vector Laboratories, #H-1000, Burlingame, USA) with 4′, 6- Diamidino-2-Phenylindole, Dihydrochloride (DAPI; Life Technologies #D1306; 1:170).

Antibodies

The following primary antibodies were used for Immunofluorescence (IF) experiments: mouse anti α-tubulin Alexa-fluor 488 conjugated (1:100; Life Technologies #322588) AURKA (1:500; Bethyl #A300-072A), pAURKA (1:100; Cell Signaling Technology #3079S), phosphorylated INCENP Ser893/Ser894 (pINCENP) (1:1000; gift from M. Lampson) (Salimian et al. 2011), Crest/ACA (1:30; Antibodies Incorporated #15–234), phosphorylated CDC25B (1:100; Signalway Antibodies #11949), γ-tubulin (1:100; Sigma-Aldrich #T6557), AURKC (1:500; Abcam #ab38298), phosphorylated AURKA/B/C (1:100; Cell Signaling Technology #2914S), MAD2 (1:100; Biolegend #PRB452C), MSY2 (1:20,000; gift from R. Schultz) (Yu, Hecht and Schultz 2002). The following secondary antibodies were used at 1:200 for IF experiments: Anti-human-Alexa-633 (Life Technologies #A21091), anti-mouse-Alexa-488 (Life Technologies #A11029), anti-rabbit-Alexa-568 (Life Technologies #A10042).

Microscopy

Images were captured using a Leica SP8 confocal microscope equipped with a 40×, 1.20 NA oil immersion objective. For each image, optical z-slices were obtained using a 1.0

μm step with a zoom setting of 4. For comparison of pixel intensities, the laser power was kept constant for each oocyte in an experiment.

To monitor the extrusion of polar bodies of oocytes, prophase I-arrested oocytes were matured *in vitro* using an EVOS FL Auto Imaging System (Life Technologies) with a 20× objective. The microscope stage was heated to 37 °C and 5% CO2 was maintained using the EVOS Onstage Incubator. Images were acquired every 20 min and processed using NIH Image J software.

Time-lapse image acquisitions were performed using Viventis LS1 Live light sheet microscope system with a Nikon 25X NA 1.1 detection objective with 1.5 x zoom and 51 2-um optical sections were taken with a 750 x 750-pixel image resolution using 10 min time intervals.

Histology

Ovaries of the female mice that were in the fertility trials were fixed in Modified Davidsons fixative solution (Electron Microscopy Sciences, #64133-50) for 6–12 h and were processed by the Office of Translational Science at Rutgers University for histology services. Five micrometer sections of paraffin embedded ovaries were stained with Harris H/E. Ovarian images were acquired at the 1^{st}, 5^{th}, and 10^{th} sections in each ovary, under a bright field microscope EVOS FL Auto Imaging System (Life Technologies) with a 20× objective and images were stitched together to project the entire ovary. Ovarian follicles were quantified using morphological criteria.

Image analysis

Image J software was used to process all images (NIH, Bethesda, USA). For analysis, z-slices for each image were merged into a projection. Bipolar spindle length was measured between the two furthest points on both spindles using the line tool in Image J. Bipolar spindle area was measured using the freehand tool to mark precisely around the spindle. Spindle marker α-tubulin was used to define the area of the spindle. For pixel intensity analyses the average pixel intensity was recorded using the measurement tool. To define the region of the chromosomes for intensity measurements, the DNA channel (DAPI) was used as a mask. MTOC markers, including AURKA and γ-tubulin were used to define spindle poles, and CREST was used as a kinetochore marker for pixel intensity measurements.

Statistical analysis

T-test and one-way analysis of variance (Anova) were used to evaluate the significant difference among data sets using Prism software (GraphPad Software). The details for each experiment can be found in the Results section as well as the figure legends. "Experimental n" refers to the number of animals used to repeat each experiment. Data is shown as the mean ± the standard error of the mean (SEM). $P < 0.05$ was considered significant.

REFERENCES

1. Agnese, V., V. Bazan, F. P. Fiorentino, D. Fanale, G. Badalamenti, G. Colucci, V. Adamo, D. Santini & A. Russo (2007) The role of Aurora-A inhibitors in cancer therapy. *Ann Oncol,* 18 Suppl 6**,** vi47-52.
2. Anand, S., S. Penrhyn-Lowe & A. R. Venkitaraman (2003) AURORA-A amplification overrides the mitotic spindle assembly checkpoint, inducing resistance to Taxol. *Cancer Cell,* 3**,** 51-62.
3. Asteriti, I. A., M. Giubettini, P. Lavia & G. Guarguaglini (2011) Aurora-A inactivation causes mitotic spindle pole fragmentation by unbalancing microtubule-generated forces. *Mol Cancer,* 10**,** 131.
4. Avo Santos, M., C. van de Werken, M. de Vries, H. Jahr, M. J. Vromans, J. S. Laven, B. C. Fauser, G. J. Kops, S. M. Lens & E. B. Baart (2011) A role for Aurora C in the chromosomal passenger complex during human preimplantation embryo development. *Hum Reprod,* 26**,** 1868-81.
5. Azoury, J., K. W. Lee, V. Georget, P. Rassinier, B. Leader & M. H. Verlhac (2008) Spindle positioning in mouse oocytes relies on a dynamic meshwork of actin filaments. *Curr Biol,* 18**,** 1514-9.
6. Balboula, A. Z., A. L. Nguyen, A. S. Gentilello, S. M. Quartuccio, D. Drutovic, P. Solc & K. Schindler (2016) Haspin kinase regulates microtubule-organizing center clustering and stability through Aurora kinase C in mouse oocytes. *J Cell Sci,* 129**,** 3648-3660.
7. Balboula, A. Z. & K. Schindler (2014) Selective disruption of aurora C kinase reveals distinct functions from aurora B kinase during meiosis in mouse oocytes. *PLoS Genet,* 10**,** e1004194.
8. Bayliss, R., T. Sardon, I. Vernos & E. Conti (2003) Structural basis of Aurora-A activation by TPX2 at the mitotic spindle. *Mol Cell,* 12**,** 851-62.
9. Bennabi, I., M. E. Terret & M. H. Verlhac (2016) Meiotic spindle assembly and chromosome segregation in oocytes. *J Cell Biol,* 215**,** 611-619.
10. Bischoff, J. R., L. Anderson, Y. Zhu, K. Mossie, L. Ng, B. Souza, B. Schryver, P. Flanagan, F. Clairvoyant, C. Ginther, C. S. Chan, M. Novotny, D. J. Slamon & G. D. Plowman (1998) A homologue of Drosophila aurora kinase is oncogenic and amplified in human colorectal cancers. *EMBO J,* 17**,** 3052-65.
11. Bischoff, J. R. & G. D. Plowman (1999) The Aurora/Ipl1p kinase family: regulators of chromosome segregation and cytokinesis. *Trends Cell Biol,* 9**,** 454-9.
12. Bishop, J. D. & J. M. Schumacher (2002) Phosphorylation of the carboxyl terminus of inner centromere protein (INCENP) by the Aurora B Kinase stimulates Aurora B kinase activity. *J Biol Chem,* 277**,** 27577-80.
13. Brar, G. A., B. M. Kiburz, Y. Zhang, J. E. Kim, F. White & A. Amon (2006) Rec8 phosphorylation and recombination promote the step-wise loss of cohesins in meiosis. *Nature,* 441**,** 532-6.
14. Breuer, M., A. Kolano, M. Kwon, C. C. Li, T. F. Tsai, D. Pellman, S. Brunet & M. H. Verlhac (2010) HURP permits MTOC sorting for robust meiotic spindle bipolarity, similar to extra centrosome clustering in cancer cells. *J Cell Biol,* 191**,** 1251-60.

15. Brown, J. R., K. K. Koretke, M. L. Birkeland, P. Sanseau & D. R. Patrick (2004) Evolutionary relationships of Aurora kinases: implications for model organism studies and the development of anti-cancer drugs. *BMC Evol Biol,* 4**,** 39.
16. Calarco, P. G. (2000) Centrosome precursors in the acentriolar mouse oocyte. *Microsc Res Tech,* 49**,** 428-34.
17. Carvajal, R. D., A. Tse & G. K. Schwartz (2006) Aurora kinases: new targets for cancer therapy. *Clin Cancer Res,* 12**,** 6869-75.
18. Chan, C. S. & D. Botstein (1993) Isolation and characterization of chromosome-gain and increase-in-ploidy mutants in yeast. *Genetics,* 135**,** 677-91.
19. Chatot, C. L., C. A. Ziomek, B. D. Bavister, J. L. Lewis & I. Torres (1989) An improved culture medium supports development of random-bred 1-cell mouse embryos in vitro. *J Reprod Fertil,* 86**,** 679-88.
20. Chiang, T., F. E. Duncan, K. Schindler, R. M. Schultz & M. A. Lampson (2010) Evidence that weakened centromere cohesion is a leading cause of age-related aneuploidy in oocytes. *Curr Biol,* 20**,** 1522-8.
21. Chiang, T., R. M. Schultz & M. A. Lampson (2011) Age-dependent susceptibility of chromosome cohesion to premature separase activation in mouse oocytes. *Biol Reprod,* 85**,** 1279-83.
22. --- (2012) Meiotic origins of maternal age-related aneuploidy. *Biol Reprod,* 86**,** 1-7.
23. Clift, D. & M. Schuh (2013) Restarting life: fertilization and the transition from meiosis to mitosis. *Nat Rev Mol Cell Biol,* 14**,** 549-62.
24. --- (2015) A three-step MTOC fragmentation mechanism facilitates bipolar spindle assembly in mouse oocytes. *Nat Commun,* 6**,** 7217.
25. Collins, J. K., S. I. R. Lane, J. A. Merriman & K. T. Jones (2015) DNA damage induces a meiotic arrest in mouse oocytes mediated by the spindle assembly checkpoint. *Nat Commun,* 6**,** 8553.
26. Cowley, D. O., J. A. Rivera-Pérez, M. Schliekelman, Y. J. He, T. G. Oliver, L. Lu, R. O'Quinn, E. D. Salmon, T. Magnuson & T. Van Dyke (2009) Aurora-A kinase is essential for bipolar spindle formation and early development. *Mol Cell Biol,* 29**,** 1059-71.
27. De Luca, M., L. Brunetto, I. A. Asteriti, M. Giubettini, P. Lavia & G. Guarguaglini (2008) Aurora-A and ch-TOG act in a common pathway in control of spindle pole integrity. *Oncogene,* 27**,** 6539-49.
28. DeLuca, J. G. (2017) Aurora A Kinase Function at Kinetochores. *Cold Spring Harb Symp Quant Biol,* 82**,** 91-99.
29. DeLuca, K. F., A. Meppelink, A. J. Broad, J. E. Mick, O. B. Peersen, S. Pektas, S. M. A. Lens & J. G. DeLuca (2018) Aurora A kinase phosphorylates Hec1 to regulate metaphase kinetochore-microtubule dynamics. *J Cell Biol,* 217**,** 163-177.
30. Du, J. & G. J. Hannon (2004) Suppression of p160ROCK bypasses cell cycle arrest after Aurora-A/STK15 depletion. *Proc Natl Acad Sci U S A,* 101**,** 8975-80.
31. Dutertre, S., M. Cazales, M. Quaranta, C. Froment, V. Trabut, C. Dozier, G. Mirey, J. P. Bouché, N. Theis-Febvre, E. Schmitt, B. Monsarrat, C. Prigent & B. Ducommun (2004) Phosphorylation of CDC25B by Aurora-A at the centrosome contributes to the G2-M transition. *J Cell Sci,* 117**,** 2523-31.

32. Eyers, P. A., E. Erikson, L. G. Chen & J. L. Maller (2003) A novel mechanism for activation of the protein kinase Aurora A. *Curr Biol,* 13**,** 691-7.
33. Field, C. M. & P. Lénárt (2011) Bulk cytoplasmic actin and its functions in meiosis and mitosis. *Curr Biol,* 21**,** R825-30.
34. Franasiak, J. M., E. J. Forman, K. H. Hong, M. D. Werner, K. M. Upham, N. R. Treff & R. T. Scott (2014) The nature of aneuploidy with increasing age of the female partner: a review of 15,169 consecutive trophectoderm biopsies evaluated with comprehensive chromosomal screening. *Fertil Steril,* 101**,** 656-663.e1.
35. Francisco, L., W. Wang & C. S. Chan (1994) Type 1 protein phosphatase acts in opposition to IpL1 protein kinase in regulating yeast chromosome segregation. *Mol Cell Biol,* 14**,** 4731-40.
36. Gassmann, R., A. Carvalho, A. J. Henzing, S. Ruchaud, D. F. Hudson, R. Honda, E. A. Nigg, D. L. Gerloff & W. C. Earnshaw (2004) Borealin: a novel chromosomal passenger required for stability of the bipolar mitotic spindle. *J Cell Biol,* 166**,** 179-91.
37. Gautschi, O., J. Heighway, P. C. Mack, P. R. Purnell, P. N. Lara & D. R. Gandara (2008) Aurora kinases as anticancer drug targets. *Clin Cancer Res,* 14**,** 1639-48.
38. Giles, F. J., J. Cortes, D. Jones, D. Bergstrom, H. Kantarjian & S. J. Freedman (2007) MK-0457, a novel kinase inhibitor, is active in patients with chronic myeloid leukemia or acute lymphocytic leukemia with the T315I BCR-ABL mutation. *Blood,* 109**,** 500-2.
39. Glover, D. M., M. H. Leibowitz, D. A. McLean & H. Parry (1995) Mutations in aurora prevent centrosome separation leading to the formation of monopolar spindles. *Cell,* 81**,** 95-105.
40. Gruhn, J. R., A. P. Zielinska, V. Shukla, R. Blanshard, A. Capalbo, D. Cimadomo, D. Nikiforov, A. C. Chan, L. J. Newnham, I. Vogel, C. Scarica, M. Krapchev, D. Taylor, S. G. Kristensen, J. Cheng, E. Ernst, A. B. Bjørn, L. B. Colmorn, M. Blayney, K. Elder, J. Liss, G. Hartshorne, M. L. Grøndahl, L. Rienzi, F. Ubaldi, R. McCoy, K. Lukaszuk, C. Y. Andersen, M. Schuh & E. R. Hoffmann (2019) Chromosome errors in human eggs shape natural fertility over reproductive life span. *Science,* 365**,** 1466-1469.
41. Guse, A., M. Mishima & M. Glotzer (2005) Phosphorylation of ZEN-4/MKLP1 by aurora B regulates completion of cytokinesis. *Curr Biol,* 15**,** 778-86.
42. Hached, K., S. Z. Xie, E. Buffin, D. Cladière, C. Rachez, M. Sacras, P. K. Sorger & K. Wassmann (2011) Mps1 at kinetochores is essential for female mouse meiosis I. *Development,* 138**,** 2261-71.
43. Handyside, A. H. (2012) Molecular origin of female meiotic aneuploidies. *Biochim Biophys Acta,* 1822**,** 1913-20.
44. Herbert, M., M. Levasseur, H. Homer, K. Yallop, A. Murdoch & A. McDougall (2003) Homologue disjunction in mouse oocytes requires proteolysis of securin and cyclin B1. *Nat Cell Biol,* 5**,** 1023-5.
45. Hirota, T., N. Kunitoku, T. Sasayama, T. Marumoto, D. Zhang, M. Nitta, K. Hatakeyama & H. Saya (2003) Aurora-A and an interacting activator, the LIM protein Ajuba, are required for mitotic commitment in human cells. *Cell,* 114**,** 585-98.

46. Homer, H. A., A. McDougall, M. Levasseur, A. P. Murdoch & M. Herbert (2005a) Mad2 is required for inhibiting securin and cyclin B degradation following spindle depolymerisation in meiosis I mouse oocytes. *Reproduction,* 130**,** 829-43.
47. Homer, H. A., A. McDougall, M. Levasseur, K. Yallop, A. P. Murdoch & M. Herbert (2005b) Mad2 prevents aneuploidy and premature proteolysis of cyclin B and securin during meiosis I in mouse oocytes. *Genes Dev,* 19**,** 202-7.
48. Jia, C. W., L. Wang, Y. L. Lan, R. Song, L. Y. Zhou, L. Yu, Y. Yang, Y. Liang, Y. Li, Y. M. Ma & S. Y. Wang (2015) Aneuploidy in Early Miscarriage and its Related Factors. *Chin Med J (Engl),* 128**,** 2772-6.
49. Kelly, A. E. & H. Funabiki (2009) Correcting aberrant kinetochore microtubule attachments: an Aurora B-centric view. *Curr Opin Cell Biol,* 21**,** 51-8.
50. Kinoshita, K., T. L. Noetzel, L. Pelletier, K. Mechtler, D. N. Drechsel, A. Schwager, M. Lee, J. W. Raff & A. A. Hyman (2005) Aurora A phosphorylation of TACC3/maskin is required for centrosome-dependent microtubule assembly in mitosis. *J Cell Biol,* 170**,** 1047-55.
51. Kitagawa, M. & S. H. Lee (2015) The chromosomal passenger complex (CPC) as a key orchestrator of orderly mitotic exit and cytokinesis. *Front Cell Dev Biol,* 3**,** 14.
52. Kitajima, T. S., M. Ohsugi & J. Ellenberg (2011) Complete kinetochore tracking reveals error-prone homologous chromosome biorientation in mammalian oocytes. *Cell,* 146**,** 568-81.
53. Kitajima, T. S., T. Sakuno, K. Ishiguro, S. Iemura, T. Natsume, S. A. Kawashima & Y. Watanabe (2006) Shugoshin collaborates with protein phosphatase 2A to protect cohesin. *Nature,* 441**,** 46-52.
54. Komrskova, P., A. Susor, R. Malik, B. Prochazkova, L. Liskova, J. Supolikova, S. Hladky & M. Kubelka (2014) Aurora kinase A is not involved in CPEB1 phosphorylation and cyclin B1 mRNA polyadenylation during meiotic maturation of porcine oocytes. *PLoS One,* 9**,** e101222.
55. Kovarikova, V., J. Burkus, P. Rehak, A. Brzakova, P. Solc & V. Baran (2016) Aurora kinase A is essential for correct chromosome segregation in mouse zygote. *Zygote,* 24**,** 326-37.
56. Kudo, N. R., K. Wassmann, M. Anger, M. Schuh, K. G. Wirth, H. Xu, W. Helmhart, H. Kudo, M. McKay, B. Maro, J. Ellenberg, P. de Boer & K. Nasmyth (2006) Resolution of chiasmata in oocytes requires separase-mediated proteolysis. *Cell,* 126**,** 135-46.
57. Kunitoku, N., T. Sasayama, T. Marumoto, D. Zhang, S. Honda, O. Kobayashi, K. Hatakeyama, Y. Ushio, H. Saya & T. Hirota (2003) CENP-A phosphorylation by Aurora-A in prophase is required for enrichment of Aurora-B at inner centromeres and for kinetochore function. *Dev Cell,* 5**,** 853-64.
58. Lara-Gonzalez, P., F. G. Westhorpe & S. S. Taylor (2012) The spindle assembly checkpoint. *Curr Biol,* 22**,** R966-80.
59. Lew, D. J. & D. J. Burke (2003) The spindle assembly and spindle position checkpoints. *Annu Rev Genet,* 37**,** 251-82.

60. Macůrek, L., A. Lindqvist, D. Lim, M. A. Lampson, R. Klompmaker, R. Freire, C. Clouin, S. S. Taylor, M. B. Yaffe & R. H. Medema (2008) Polo-like kinase-1 is activated by aurora A to promote checkpoint recovery. *Nature,* 455**,** 119-23.
61. Maddox, A. S., J. Azoury & J. Dumont (2012) Polar body cytokinesis. *Cytoskeleton (Hoboken),* 69**,** 855-68.
62. Magnaghi-Jaulin, L., G. Eot-Houllier, E. Gallaud & R. Giet (2019) Aurora A Protein Kinase: To the Centrosome and Beyond. *Biomolecules,* 9.
63. Marumoto, T., S. Honda, T. Hara, M. Nitta, T. Hirota, E. Kohmura & H. Saya (2003) Aurora-A kinase maintains the fidelity of early and late mitotic events in HeLa cells. *J Biol Chem,* 278**,** 51786-95.
64. Menasha, J., B. Levy, K. Hirschhorn & N. B. Kardon (2005) Incidence and spectrum of chromosome abnormalities in spontaneous abortions: new insights from a 12-year study. *Genet Med,* 7**,** 251-63.
65. Mihajlović, A. I. & G. FitzHarris (2018) Segregating Chromosomes in the Mammalian Oocyte. *Curr Biol,* 28**,** R895-R907.
66. Mori, D., Y. Yano, K. Toyo-oka, N. Yoshida, M. Yamada, M. Muramatsu, D. Zhang, H. Saya, Y. Y. Toyoshima, K. Kinoshita, A. Wynshaw-Boris & S. Hirotsune (2007) NDEL1 phosphorylation by Aurora-A kinase is essential for centrosomal maturation, separation, and TACC3 recruitment. *Mol Cell Biol,* 27**,** 352-67.
67. Musacchio, A. & A. Ciliberto (2012) The spindle-assembly checkpoint and the beauty of self-destruction. *Nat Struct Mol Biol,* 19**,** 1059-61.
68. Nagaoka, S. I., T. J. Hassold & P. A. Hunt (2012) Human aneuploidy: mechanisms and new insights into an age-old problem. *Nat Rev Genet,* 13**,** 493-504.
69. Nguyen, A. L., D. Drutovic, B. N. Vazquez, W. El Yakoubi, A. S. Gentilello, M. Malumbres, P. Solc & K. Schindler (2018) Genetic Interactions between the Aurora Kinases Reveal New Requirements for AURKB and AURKC during Oocyte Meiosis. *Curr Biol,* 28**,** 3458-3468.e5.
70. Niault, T., K. Hached, R. Sotillo, P. K. Sorger, B. Maro, R. Benezra & K. Wassmann (2007) Changing Mad2 levels affects chromosome segregation and spindle assembly checkpoint control in female mouse meiosis I. *PLoS One,* 2**,** e1165.
71. Oliver, T. R., E. Feingold, K. Yu, V. Cheung, S. Tinker, M. Yadav-Shah, N. Masse & S. L. Sherman (2008) New insights into human nondisjunction of chromosome 21 in oocytes. *PLoS Genet,* 4**,** e1000033.
72. Orr, B., K. M. Godek & D. Compton (2015) Aneuploidy. *Curr Biol,* 25**,** R538-42.
73. Petracchi, F., D. S. Colaci, L. Igarzabal & E. Gadow (2009) Cytogenetic analysis of first trimester pregnancy loss. *Int J Gynaecol Obstet,* 104**,** 243-4.
74. Pinyol, R., J. Scrofani & I. Vernos (2013) The role of NEDD1 phosphorylation by Aurora A in chromosomal microtubule nucleation and spindle function. *Curr Biol,* 23**,** 143-9.
75. Reboutier, D., C. Benaud & C. Prigent (2015) Aurora A's Functions During Mitotic Exit: The Guess Who Game. *Front Oncol,* 5**,** 290.
76. Roeles, J. & G. Tsiavaliaris (2019) Actin-microtubule interplay coordinates spindle assembly in human oocytes. *Nat Commun,* 10**,** 4651.

77. Salimian, K. J., E. R. Ballister, E. M. Smoak, S. Wood, T. Panchenko, M. A. Lampson & B. E. Black (2011) Feedback control in sensing chromosome biorientation by the Aurora B kinase. *Curr Biol,* 21**,** 1158-65.
78. Santaguida, S., C. Vernieri, F. Villa, A. Ciliberto & A. Musacchio (2011) Evidence that Aurora B is implicated in spindle checkpoint signalling independently of error correction. *EMBO J,* 30**,** 1508-19.
79. Saskova, A., P. Solc, V. Baran, M. Kubelka, R. M. Schultz & J. Motlik (2008) Aurora kinase A controls meiosis I progression in mouse oocytes. *Cell Cycle,* 7**,** 2368-76.
80. Schuh, M. & J. Ellenberg (2007) Self-organization of MTOCs replaces centrosome function during acentrosomal spindle assembly in live mouse oocytes. *Cell,* 130**,** 484-98.
81. Schumacher, J. M., N. Ashcroft, P. J. Donovan & A. Golden (1998a) A highly conserved centrosomal kinase, AIR-1, is required for accurate cell cycle progression and segregation of developmental factors in Caenorhabditis elegans embryos. *Development,* 125**,** 4391-402.
82. Schumacher, J. M., A. Golden & P. J. Donovan (1998b) AIR-2: An Aurora/Ipl1-related protein kinase associated with chromosomes and midbody microtubules is required for polar body extrusion and cytokinesis in Caenorhabditis elegans embryos. *J Cell Biol,* 143**,** 1635-46.
83. Sen, S., H. Zhou & R. A. White (1997) A putative serine/threonine kinase encoding gene BTAK on chromosome 20q13 is amplified and overexpressed in human breast cancer cell lines. *Oncogene,* 14**,** 2195-200.
84. Shindo, M., H. Nakano, H. Kuroyanagi, T. Shirasawa, M. Mihara, D. J. Gilbert, N. A. Jenkins, N. G. Copeland, H. Yagita & K. Okumura (1998) cDNA cloning, expression, subcellular localization, and chromosomal assignment of mammalian aurora homologues, aurora-related kinase (ARK) 1 and 2. *Biochem Biophys Res Commun,* 244**,** 285-92.
85. Shuda, K., K. Schindler, J. Ma, R. M. Schultz & P. J. Donovan (2009) Aurora kinase B modulates chromosome alignment in mouse oocytes. *Mol Reprod Dev,* 76**,** 1094-105.
86. Solc, P., V. Baran, A. Mayer, T. Bohmova, G. Panenkova-Havlova, A. Saskova, R. M. Schultz & J. Motlik (2012) Aurora kinase A drives MTOC biogenesis but does not trigger resumption of meiosis in mouse oocytes matured in vivo. *Biol Reprod,* 87**,** 85.
87. Solc, P., T. S. Kitajima, S. Yoshida, A. Brzakova, M. Kaido, V. Baran, A. Mayer, P. Samalova, J. Motlik & J. Ellenberg (2015) Multiple requirements of PLK1 during mouse oocyte maturation. *PLoS One,* 10**,** e0116783.
88. Soler, A., C. Morales, I. Mademont-Soler, E. Margarit, A. Borrell, V. Borobio, M. Muñoz & A. Sánchez (2017) Overview of Chromosome Abnormalities in First Trimester Miscarriages: A Series of 1,011 Consecutive Chorionic Villi Sample Karyotypes. *Cytogenet Genome Res,* 152**,** 81-89.
89. Sudakin, V., G. K. Chan & T. J. Yen (2001) Checkpoint inhibition of the APC/C in HeLa cells is mediated by a complex of BUBR1, BUB3, CDC20, and MAD2. *J Cell Biol,* 154**,** 925-36.

90. Sun, S. C. & N. H. Kim (2013) Molecular mechanisms of asymmetric division in oocytes. *Microsc Microanal,* 19**,** 883-97.
91. Szollosi, D., P. Calarco & R. P. Donahue (1972) Absence of centrioles in the first and second meiotic spindles of mouse oocytes. *J Cell Sci,* 11**,** 521-41.
92. Terret, M. E., K. Wassmann, I. Waizenegger, B. Maro, J. M. Peters & M. H. Verlhac (2003) The meiosis I-to-meiosis II transition in mouse oocytes requires separase activity. *Curr Biol,* 13**,** 1797-802.
93. Vader, G., A. F. Maia & S. M. Lens (2008) The chromosomal passenger complex and the spindle assembly checkpoint: kinetochore-microtubule error correction and beyond. *Cell Div,* 3**,** 10.
94. Vallot, A., I. Leontiou, D. Cladière, W. El Yakoubi, S. Bolte, E. Buffin & K. Wassmann (2018) Tension-Induced Error Correction and Not Kinetochore Attachment Status Activates the SAC in an Aurora-B/C-Dependent Manner in Oocytes. *Curr Biol,* 28**,** 130-139.e3.
95. van der Waal, M. S., R. C. Hengeveld, A. van der Horst & S. M. Lens (2012) Cell division control by the Chromosomal Passenger Complex. *Exp Cell Res,* 318**,** 1407-20.
96. Willems, E., M. Dedobbeleer, M. Digregorio, A. Lombard, P. N. Lumapat & B. Rogister (2018) The functional diversity of Aurora kinases: a comprehensive review. *Cell Div,* 13**,** 7.
97. Wollman, R., E. N. Cytrynbaum, J. T. Jones, T. Meyer, J. M. Scholey & A. Mogilner (2005) Efficient chromosome capture requires a bias in the 'search-and-capture' process during mitotic-spindle assembly. *Curr Biol,* 15**,** 828-32.
98. Yang, H., T. Burke, J. Dempsey, B. Diaz, E. Collins, J. Toth, R. Beckmann & X. Ye (2005) Mitotic requirement for aurora A kinase is bypassed in the absence of aurora B kinase. *FEBS Lett,* 579**,** 3385-91.
99. Yao, L. J., Z. S. Zhong, L. S. Zhang, D. Y. Chen, H. Schatten & Q. Y. Sun (2004) Aurora-A is a critical regulator of microtubule assembly and nuclear activity in mouse oocytes, fertilized eggs, and early embryos. *Biol Reprod,* 70**,** 1392-9.
100. Yi, K. & R. Li (2012) Actin cytoskeleton in cell polarity and asymmetric division during mouse oocyte maturation. *Cytoskeleton (Hoboken),* 69**,** 727-37.
101. Yu, J., N. B. Hecht & R. M. Schultz (2002) RNA-binding properties and translation repression in vitro by germ cell-specific MSY2 protein. *Biol Reprod,* 67**,** 1093-8.
102. Zhai, R., Y. F. Yuan, Y. Zhao, X. M. Liu, Y. H. Zhen, F. F. Yang, L. Wang, C. Z. Huang, J. Cao & L. J. Huo (2013) Bora regulates meiotic spindle assembly and cell cycle during mouse oocyte meiosis. *Mol Reprod Dev,* 80**,** 474-87.
103. Zhang, X., S. C. Ems-McClung & C. E. Walczak (2008) Aurora A phosphorylates MCAK to control ran-dependent spindle bipolarity. *Mol Biol Cell,* 19**,** 2752-65.
104. Zhou, H., J. Kuang, L. Zhong, W. L. Kuo, J. W. Gray, A. Sahin, B. R. Brinkley & S. Sen (1998) Tumour amplified kinase STK15/BTAK induces centrosome amplification, aneuploidy and transformation. *Nat Genet,* 20**,** 189-93.